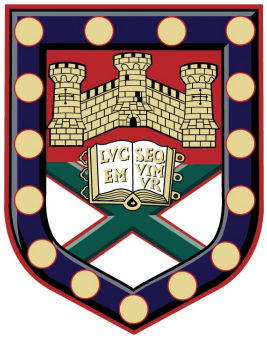

Rate-induced transitions for parameter shift systems

Submitted by

Hassan Mazin Alkhayuon

to the University of Exeter as a thesis for the degree of Doctor of Philosophy in Mathematics, July 2018.

I certify that all material in this thesis which is not my own work has been identified and that no material has previously been submitted and approved for the award of a degree by this or any other University.

.....

Hassan Alkhayuon

Abstract

Rate-induced transitions have recently emerged as an identifiable type of instability of attractors in nonautonomous dynamical systems. In most studies so far, these attractors can be associated with equilibria of an autonomous limiting system, but this is not necessarily the case. For a specific class of systems with a parameter shift between two autonomous systems, we consider how the breakdown of the quasistatic approximation for attractors can lead to rate-induced transitions, where nonautonomous instability can be characterised in terms of a critical rate of the parameter shift.

We find a number of new phenomena for non-equilibrium attractors: *weak tracking* where the pullback attractor of the system limits to a proper subset of the attractor of the future limit system, *partial tipping* where certain phases of the pullback attractor tip and others track the quasistatic attractor, *invisible tipping* where the critical rate of partial tipping is isolated and separates two parameter regions where the system exhibits end-point tracking.

For a model parameter shift system with periodic attractors, we characterise thresholds of rate-induced tipping to partial and total tipping. We show these thresholds can be found in terms of certain periodic-to-periodic and periodic-to-equilibrium connections that we determine using Lin's method for an augmented system.

Considering weak tracking for a nonautonomous Rössler system, we show that there are infinitely many critical rates at which a pullback attracting solution of the system tracks an embedded unstable periodic orbit of the future chaotic attractor.

Acknowledgments

I would like to express my deepest appreciation to my supervisor Peter Ashwin for his valuable support, his expert guidance and for his patience and constructive criticism. During the three years of my PhD, Peter has taught me by example how to be organised and effective. He dedicated a great deal of effort to help me build up my research skills, and I owe him a great debt of gratitude.

I would like to extend my thanks to my second supervisor Mark Holland and my academic assessors Jan Sieber and Dalia Terhesiu for their helpful comments and feedback at various stages of my work. Also, I am very grateful for my personal tutor Ana Rodrigues for her support and guidance.

My office mates Paul Ritchie, Damian Smug, and Courtney Quinn have made the working environment very enjoyable. They have been a great help in many different ways: with MATLAB and LaTex, proofreading my writing, reviewing my presentations and even double-checking my mathematics on different occasions.

During my PhD I have benefited from valuable discussions with Sebastian Wieczorek, Martin Rasmussen, Bernd Krauskopf, Ulrike Feudel, Chun Xie, Oskar Weinberger, Pedro Peres, Sohaib Hasan, Karl Newman, Sabiha Majumder, Salah Hamza Abid, Richard Wood and James Yorke. I am also thankful to Tsnem Salhy for her artistic comments that helped me improve Figures 5.1, 5.2,5.3, 5.4, 6.3 and to Zahraa Abdalhussain for the inspiring discussions that helped me improving some of my codes.

I am very thankful to my flatmates Atheer F. Al-Anbaki and Azzam Aladool

for the great time we spent, the very competitive board games we played and the delicious food we shared.

I also would like to express my thanks to my parents Jinan and Mazin for their extraordinary support and encouragement, to my aunt Liqaa and my cousin Lara for showing their interest in my research on different occasions.

Finally, I would like to acknowledge the generous funding of my PhD program by the Higher Committee for Education Development in Iraq (HCED Iraq), grant agreement No. D13436.

Contents

List of Figures

Chapter 1

Introduction

"*Tipping points*" or "*critical transitions*" are sudden and unexpected changes in the behaviour of a system subject to relatively small changes in its input [39]. These changes are often catastrophic and even irreversible, i.e. their long-term consequences cannot be prevented by simply reversing its input level to the previous state.

Since Malcolm Gladwell published his book [21] in 2000, the use of the term "tipping point" in the scientific literature has risen exponentially [79]. Since then, many problems in climate science [39, 73, 16], ecology [72, 71, 15, 49], finance [48, 81], and biology [54] have been usefully looked at in terms of tipping points. We refer to Feudel *et al* [19] for an extensive review of the applications of tipping in natural science.

On the mathematical side, various techniques have been developed and used to describe mechanisms associated with tipping phenomena. For example, Kuehn [35, 36], has provided a mathematical framework to describe tipping in the presence of noise using fast-slow systems theory. Wieczorek *et al* [80] and Ashwin *et al* [5] have studied tipping for single time-scale systems using a so-called *quasistatic* approximation.

Bifurcation theory plays a significant role in understanding tipping [77, 78]. We

say a system has a bifurcation point at some parameter value if this value separates two regions of qualitatively different behaviour [37]. In some cases, tipping behaviour is associated with a fold bifurcation where branches of stable and unstable equilibria meet, see Figure 1.1. Although *bifurcation-induced tipping* can be seen in many ecosystem models [70, 45], bifurcation is not the only mechanism that might be called tipping. For example, a solution of a noisy bistable system can switch from tracking one stable state to the other forced through a fluctuation of noise. This type of tipping is called *noise-induced tipping* in [5, Section 4].

In their work [44], Luke and Cox show that their carbon-temperature model can exhibit tipping behaviour or "compost-bomb instability" when the heat generated by decomposition of plant matter within the soil increases more quickly than it can escape. In this case, the tipping may not be associated with a critical value of a parameter. Instead, it can depend on how fast the parameter is changing. A similar idea was discussed in [80]. In 2012, *rate-dependent tipping* was introduced by Ashwin *et al* [5] while identifying three mechanisms that can independently cause tipping:

- **Bifurcation-induced tipping (B-tipping)**: This occurs when the system passes through a bifurcation point.
- **Noise-induced tipping (N-tipping)**: This occurs when the solution of a bistable (multistable) system switches randomly between stable states.
- **Rate-induced tipping (R-tipping)**: This occurs when the system fails to track a continuously changing quasi-static attractor.

Whilst bifurcation theory and probability theory provide many useful techniques to understand and analyse B- and N-tipping, R-tipping is relatively less explored. For example, the only systems that have been considered in detail are systems with moving equilibrium attractors. This thesis addresses R-tipping (and the related phenomena) from general attractors for a specific class of systems with a parameter shift between two autonomous systems.

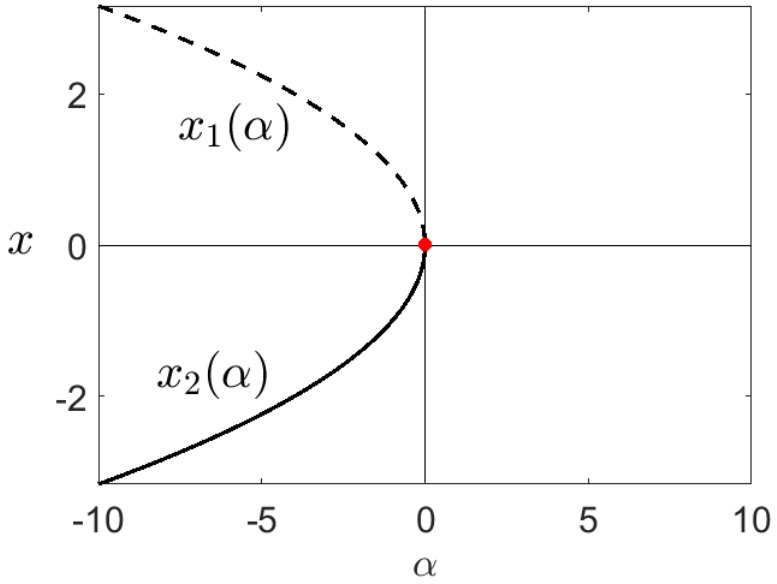

Figure 1.1: Fold bifurcation in the phase-parameter plane of system (1.1), after [37, Figure 3.3]. The solid line represents the stable equilibrium $x_2(\alpha)$ whilst the dashed line represents the unstable equilibrium $x_1(\alpha)$.

1.1 Bifurcation-induced tipping in simple ecological model

One of the simplest bifurcations for flows is the fold bifurcation where two branches of equilibria (one stable and the other not) meet each other at a fold. A fold bifurcation, also known as saddle-node bifurcation, can appear in one-dimensional systems on varying one parameter, and its normal form is given by [37]:

$$\dot{x} = \alpha + x^2 \tag{1.1}$$

where $\alpha, x \in \mathbb{R}$. This system has no equilibria for $\alpha > 0$ and two equilibria for $\alpha < 0$ these are $x_1 = \sqrt{-\alpha}$ and $x_2 = -\sqrt{-\alpha}$. Both of the equilibria are hyperbolic, x_2 is stable whilst x_1 is unstable. At $\alpha = 0$ the system has one nonhyperbolic equilibrium $x_0 = 0$, see Figure 1.1.

Generic conditions to identify fold bifurcation can be found in [22, Theorem 8.2].

Assume that a system $\dot{x} = f(x, \alpha)$ satisfies $f(0,0) = f_x(0,0) = 0$. Then in order to have fold bifurcation at $(0,0)$ the system must satisfy:

$$f_\alpha(0,0) \neq 0 \quad \text{and} \quad f_{xx}(0,0) \neq 0$$

where f_α, f_x are the partial derivatives of f with respect to α and x respectively.

Systems with a fold bifurcation can exhibit B-tipping due to the slow passage through the bifurcation point. Mathematical ecologist Robert May [47] introduced a simple example that has tipping induced by fold bifurcation:

$$\dot{x} = x(1-x) - \frac{\gamma x^2}{\alpha + x^2}. \tag{1.2}$$

System (1.2) can be thought of as a representation of a population dynamics $x(t)$ subject to a harvesting rate γ. The first term of (1.2) can be thought of as the growth term and the second term represents the death rate of the population $x(t)$.

Figure 1.2 shows that for $\alpha = 0.1$ the system has a bistable region for $\gamma \in (0.1787, 0.2604)$. When γ is allowed to vary linearly and slowly in time from 0 to 0.5, trajectories track the upper branch of equilibria up to the fold where the branch loses its stability at the upper fold point which cause the trajectories to jump onto the lower branch.

After the solution passes the upper fold, reducing γ to the previous level will not necessarily allow the solution to go back to track the upper branch. It has to pass through the other fold in order for a new transition to occur. For (1.2) the transition is completely reversible as long as the harvesting parameter γ can be reduced beyond 0.1787. However, the transition is catastrophic in the sense that reducing the harvesting parameter to the same level cannot help the population $x(t)$ to recover and jump back to the upper branch.

This example illustrates a bifurcation-induced tipping where the system tips whenever the parameter γ passes through a bifurcation point regardless of how fast

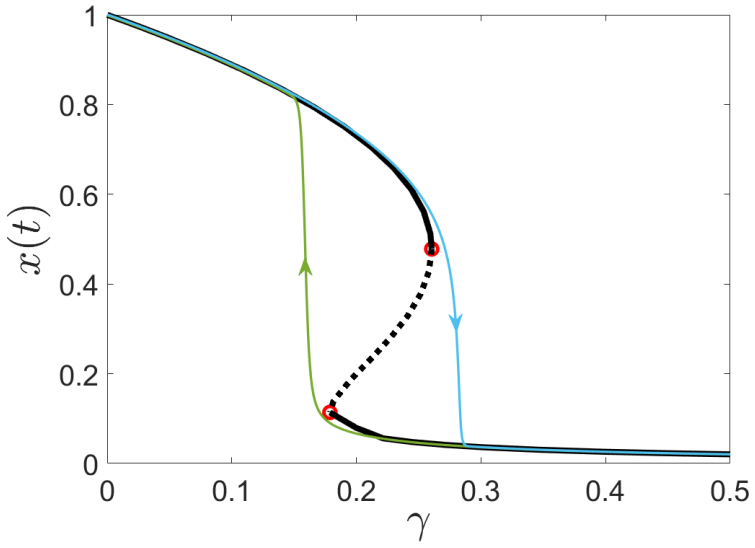

Figure 1.2: The bifurcation diagram of (1.2) contains three branches of equilibria, two of them are stable (solid black curves) and the other one is unstable (dashed black). The red circles represent the fold bifurcation points. The three branches and bifurcation points are calculated by Xppaut software [17] for $\alpha = 0.1$. To produce the blue and green curves we vary the harvesting rate γ slowly and linearly in time with constant rate $r = 0.001$. For the blue curve, we vary γ from 0 to 0.5 and start with an initial condition very close to the upper stable equilibrium. The green curve is produced by reducing γ from 0.5 to 0 and starting with an initial condition very close to the lower stable equilibrium. It can be seen that once the solution passes through the fold it will track another stable branch of equilibria. Reducing γ cannot fix the situation immediately as the solution need to pass through the other fold point in order to get back to the previous stable branch.

the passing through is. Section 1.2 considers two example of R-tipping where the speed of changing a parameter causes the transition.

1.2 Rate-induced tipping: two model examples

Since the publication of [5], several papers have been published concerning R-tipping. In order to analyse R-tipping in multi-timescale systems, Perryman and Wieczorek [57, 56] used singular perturbation techniques, such as folded singularity and canard trajectories to show the existence of so-called *non-obvious* thresholds.

Additionally, Ritchie and Sieber [63, 61] tackled the problem of providing *early warning signals* for R-tipping for systems that have noise involved. Early warning

signals (EWSs) can be defined as statistical indicators that can be used to predict the occurrence of tipping by looking at time series data [39, 63]. Although many studies have tackled the problem of providing EWSs for B-tipping, see for example [14, 16, 78, 65], EWSs for R-tipping have not been studied to the same depth. Ritchie and Sieber [63] show that a sudden increase of the autocorrelation and variance for a time series data can be considered as a warning of approaching R-tipping. Other work of Ritchie and Sieber [64] has measured the probability of having R-tipping for the same setting.

A particular context where one can investigate R-tipping is for systems of the form:

$$\dot{x} = f(x, \Lambda(rt)), \tag{1.3}$$

where $r > 0$, $x \in \mathbb{R}^n$, $\Lambda : \mathbb{R} \to \mathbb{R}$ and $f : \mathbb{R}^n \times \mathbb{R}^d \to \mathbb{R}^n$ are sufficiently smooth functions. It is useful to define a so-called *quasi-static equilibrium (attractor)* [80, 5], QSE (QSA) for short. For any fixed value of $r > 0$, if there is a set valued function $A : \mathbb{R} \to \mathbb{R}^n$ such that $A(\lambda)$ is an attractor of the system

$$\dot{x} = f(x, \lambda), \tag{1.4}$$

then $A(\lambda)$ is called a QSA of (1.3). Note that, $A(\lambda)$ is typically not stationary for any $r > 0$. Although, $A(\lambda)$ is not an attractor for (1.3), it is useful approximation of the behaviour of the system. Breaking this approximation can be viewed as rate-induced bifurcation. We illustrate this now with two examples.

1.2.1 Example 1: R-tipping from equilibrium to equilibrium

Consider the normal form of fold bifurcation with linear forcing as follows:

$$\begin{aligned} \dot{x} &= (x + \Lambda)^2 - \mu \\ \dot{\Lambda} &= r \end{aligned} \tag{1.5}$$

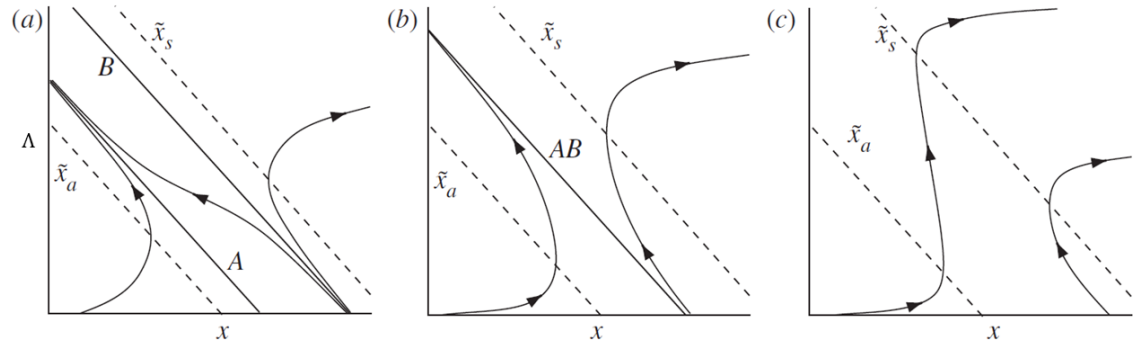

Figure 1.3: Phase portraits of (1.5). The two quasi-static equilibria $\tilde{x}_a$ and $\tilde{x}_s$ are indicated as dashed line. the invariant lines A and B are solid black. In (a) $0 < r < \mu$, (b) $r = \mu$ and (c) $r > \mu$. The figure is taken from [5, Figure 3].

This example is analysed by Ashwin *et al* [5]. For fixed $\mu > 0$ there are two quasi-static equilibria. These are:

$$\tilde{x}_a(\mu) = \{(x, \Lambda) \in \mathbb{R}^2 : \Lambda = -\sqrt{\mu} - x\}, \tag{1.6}$$

which is a stable QSE, and

$$\tilde{x}_s(\mu) = \{(x, \Lambda) \in \mathbb{R}^2 : \Lambda = \sqrt{\mu} - x\}, \tag{1.7}$$

which is unstable. By assuming $\mu > r > 0$ and considering (1.6) and (1.7) we get:

$$r = \dot{\Lambda} = -\dot{x} = -(x + \Lambda)^2 + \mu,$$

which defines two invariant lines, one attracting

$$A(\mu, r) = \{(x, \Lambda) \in \mathbb{R}^2 : \Lambda = -\sqrt{\mu - r} - x\}$$

and one repelling

$$B(\mu, r) = \{(x, \Lambda) \in \mathbb{R}^2 : \Lambda = \sqrt{\mu - r} - x\}.$$

Note that initial conditions below $B(\mu, r)$ converge to $A(\mu, r)$ whilst those above $B(\mu, r)$ rapidly blow-up to infinity. We define the threshold of R-tipping of a trajectory as the value of r at which that trajectory blows-up to infinity. Therefore, if an initial condition (x_0, Λ_0), at $t = 0$, lies between $\Lambda = -x$ and $\tilde{x}_s(\mu)$, i.e. $-x_0 < \Lambda_0 < -x_0 + \sqrt{\mu}$, then R-tipping happens when $B(\mu, r)$ crosses the initial point (x_0, Λ_0), i.e:

$$\begin{aligned} \Lambda_0 &= \sqrt{\mu - r} - x_0, \\ r &= \mu - (\Lambda_0 + x_0)^2. \end{aligned}$$

For (x_0, Λ_0) anywhere else, i.e. $\Lambda \leq -x_0$, the tipping take place when $A(\mu, r)$ and $B(\mu, r)$ coalesce into one line, which happens when $\mu = r$, we can compute the critical rate of R-tipping as:

$$r_c = \begin{cases} \mu - (\Lambda_0 + x_0)^2. & \text{if } -x_0 < \Lambda_0 < -x_0 + \sqrt{\mu} \\ \mu & \text{if } \lambda_0 \leq -x_0, \end{cases}$$

Figure 1.3 shows different scenarios for different values of r.

1.2.2 Example 2: R-tipping from equilibrium to periodic orbit

Consider the following system of ODEs:

$$\dot{z} = F(z - \Lambda(rt)), \tag{1.8}$$

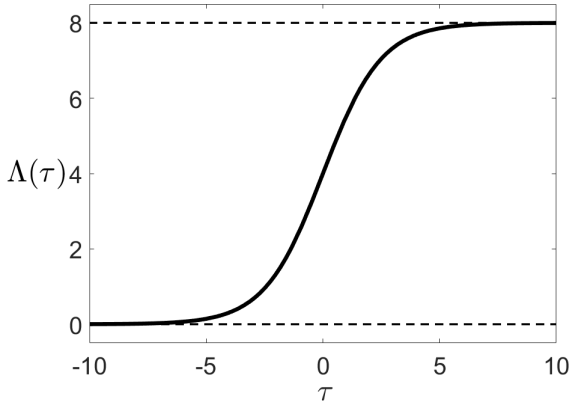

Figure 1.4: The behaviour of $\Lambda(\tau)$ for system (1.8). It can be seen that $\Lambda(\tau)$ is asymptotic to 0 and $\lambda_{\max} = 8$ as τ tends to $-\infty$ and ∞ respectively.

where $z = x + iy \in \mathbb{C}$, $\Lambda(\tau) = \lambda_{\max}(\tanh(\tau\lambda_{\max}) + 1)/2$ asymptotic to 0 as $\tau \to -\infty$ and to $\lambda_{\max}$ as $\tau \to \infty$ and

$$F(z) = (-1 + i\omega)z + |z|^2 z. \tag{1.9}$$

for ω, r and $\lambda_{\max} \in \mathbb{R}$, $r, \lambda_{\max} > 0$. The forcing term Λ behaves like a logistical growth, see Figure 1.4. Moreover, for $\Lambda = 0$ system (1.8) can be thought of as the normal form of a subcritical Hopf bifurcation.

This example was analysed first in [5] and later in more detail in [57, Section 4.3.3]. System (1.8) has a stable quasi-static equilibria that is given by $Z(\Lambda) = \Lambda + 0i$, and unstable quasi-static periodic orbit given by $\Gamma(\Lambda) = \{z \in \mathbb{C} : |z - \Lambda| < 1\}$.

For some range of values of $r > 0$ and any initial condition in the neighbourhood $\{z \in \mathbb{C} : |z| < 1\}$ solutions track $Z(\Lambda)$ (this is proved for more general setting in Theorem 4.3.1). However, there is a threshold $r_c > 0$ at which the solutions no longer tracks $Z(\Lambda)$. For $\lambda_{\max} = 8$ and $\omega = 5$ this critical rate is $r_c \approx 0.274$ [5], see the simulation in Figure 1.5.

Moreover, Ashwin *et al* [5] have pointed out that the critical rate is associated with equilibrium-to-periodic (EtoP) orbit connection for an augmented system. The

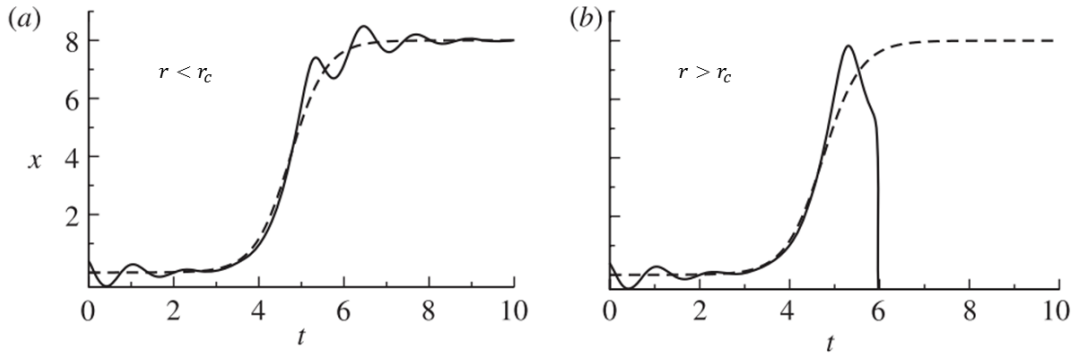

Figure 1.5: Simulations of (1.8) show R-tipping. The values of the parameters are, $\lambda_{\max} = 8, \omega = 5$, (a) $r = 0.279$, (b) $r = 0.3$. The black dashed line is the QSE $Z(\Lambda)$ and the solid black line is a trajectory with initial condition $(0.4, 0.5, 0.0001)$. The figure is taken from [5, Figure 5].
Note that: In [5, Figure 5] they stated that the values of r in (a) and (b) are 4.76 and 4.8 respectively. However, this is rather the maximum value of $\frac{d\Lambda}{dt}$ which equals to $\frac{\lambda_{\max}^2 r}{4}$. The associated values of r should in fact be 0.274 and 0.3 respectively.

augmented system can be given as:

$$\begin{aligned} \dot{z} &= F(z - \Lambda) \\ \dot{\Lambda} &= r\Lambda(\lambda_{\max} - \Lambda). \end{aligned} \tag{1.10}$$

The desired connection is between the saddle equilibrium $Z_- = (0, 0)$ and the saddle periodic orbit $\Gamma_+ = \{z \in \mathbb{C} : |z - \lambda_{\max}| < 1\}$. Perryman [57, Section 4.3.3] used Lin's method to calculate and continue this critical threshold in (r, ω)-plane.

1.3 Nonautonomous stability and R-tipping

Nonautonomous stability theory can be a useful tool for studying rate-dependent phenomena. Ashwin *et al* [4] proposed a framework for rate-induced tipping for system (1.3), with strict assumptions on $\Lambda(rt)$ that allow (1.3) to be asymptotic to different autonomous systems forward and backward in time. They call this particular class of systems *parameter shift* systems.

Ashwin *et al* used the notion of pullback attractivity to define R-tipping and provide the following scenario. Firstly, they proved that any quasi-static stable

equilibrium $X(\Lambda(rt))$ for (1.3) is associated with a *pullback attracting solution* $\tilde{x}_{pb}$. Secondly, regardless of the parameter shift $\Lambda(rt)$ the pullback attractor $\tilde{x}_{pb}$ remains close to $X(\Lambda(rt))$ for a range of small positive values of r. Finally, if there is a value r_c at which the pullback attractor $\tilde{x}_{pb}$ no longer tracks $X(\Lambda(rt))$ then this r_c called critical rate of tipping and the system has R-tipping at this value. See Section 3.2 for more detail.

The results of Ashwin *et al* [4] apply to systems where the attractors are simply equilibria. One of the aims of this thesis is to generalise these results for a wider range of attractors.

Li *et al* [42] argue that passing through fold bifurcation does not necessarily mean the system has undergone catastrophic tipping. Assume that a system in the form of (1.3) undergoes dynamic fold bifurcation at $t = \hat{\tau}$. Furthermore, assume that (1.3) undergoes critical transition at $t = \tau^*$. Li *et al* used the concept of pullback attractor to argue that τ^* is always greater than $\hat{\tau}$ and there is a time window $\tau^* - \hat{\tau}$ during which the transition is preventable by rapid reversal of $\Lambda(rt)$. Ritchie *et al* [62] have confirmed Li *et al*'s results by providing an estimation for how rapid should be the reversal of $\Lambda(rt)$ in order to prevent tipping.

Rate-induced phenomena can be related to changes in the attracting/repelling properties of an invariant set. This qualitative change is called *finite-time bifurcation* for autonomous systems [60]. Hoyer-Leitzel *et al* [26] have used this idea to investigate R-tipping. Given a time-dependent trajectory, one can quantify its attractivity along finite time-intervals by considering finite time Lyapunov exponents (FTLEs). In this case, R-tipping can be associated with switching from positive to negative FTLEs or vice versa [26].

1.4 Thesis outline

Most studies so far have only considered R-tipping for systems where all attractors are equilibria. In this thesis, we study rate-induced transitions for more general attractors. In doing so, we consider parameter shift systems [4].

In Chapter 2, we review results from the nonautonomous theory of dynamical systems. In particular, we review the notions of nonautonomous invariance and the limits of set-valued sequences. Additionally, two classes of nonautonomous dynamical systems are reviewed and illustrated with examples: these are asymptotically autonomous systems and parameter shift systems.

Chapter 3 reviews the concept of local pullback attractor and its role in understanding rate-induced transitions. The new Proposition 3.1.1 and Example 3.1.2 discuss the relationship between two different definitions of local pullback attractors, namely [4, Definition 2.3] and [30, Definition 3.48].

Chapter 4 discusses attractivity and asymptotic behaviour of parameter shift systems. We generalise some results from [4] to compact attractors in general (not necessarily equilibria). Using these results we propose general definitions of rate-induced transitions. We identify a number of new phenomena that we call *partial tipping*, *weak tracking* and *invisible tipping*.

Chapter 5 illustrates some of these phenomena in a model example with a branch of periodic attractors. Namely, system (5.1) exhibits all of partial tipping, total tipping, invisible tipping and strong tracking. For this example, we prove that the thresholds of each of these phenomena can be characterised using heteroclinic connections from periodic orbit to equilibria (PtoE) or from periodic orbit to periodic orbit (PtoP). We use Lin's method to calculate these connections and continue them in the two-parameter plane.

In Chapter 6 we presented two systems that are shown to exhibit weak tracking. Whilst system (6.1) is non-generically designed to have non-minimal attractors for the past and the future limit systems, The future attractor of system (6.5) is non-

minimal invariant set that has no proper sub-attractor (i.e non-minimal invariant but minimal attractor). One of our key observations for system (6.5) is that it has a dense set of critical rates at each of which the system exhibits weak tracking. We use a novel numerical approach based on shooting algorithm and carefully chosen Poincaré section to investigate these critical rates.

Further discussions and conclusions are provided in Chapter 7. Materials in Chapters 4 and 5 has been published in *Chaos* [1]:

> Hassan M. Alkhayuon and Peter Ashwin. Rate-induced tipping from periodic attractors: Partial tipping and connecting orbits. *Chaos: An Interdisciplinary Journal of Nonlinear Science*, 28(3):033608, Mar 2018.

Chapter 2

Nonautonomous dynamical systems

In some natural sciences, such as classical physics, it is assumed that the future state of a system can be predicted based on its present state. In other words, the changing over time is subjected to deterministic rules. This scientific principle formulates the base for the autonomous theory of dynamical systems, which is a useful representation of many real-world phenomena. However, it is limited and does not apply in some cases. Real-world systems often have external inputs that are difficult to model mathematically. In order to deal with that, mathematicians have developed a theory of nonautonomous dynamical systems (NDSs). This assumes that systems may have time-dependent forcing that can vary at a different time-scale to that of the state variables.

The autonomous theory of dynamical systems is well established: many techniques have been developed and general properties are understood. For example, there are many textbooks that discuss autonomous systems, their asymptotic behaviour and their bifurcations, such as [2, 22, 37, 55]. On the other hand, that is not the case with nonautonomous systems where the theory is less devolved and much need to be understood. Nevertheless, we mention two valuable attempts to

establish a theory for NDSs, these are [30, 58].

Although time-dependent (nonautonomous) differential equations have been studied relatively earlier, the abstract formulations of NDS have been introduced in the 1960s by George Sell [75, 74]. *Skew product flows* formulation views NDSs as ADSs on the extended phase space. Usually, this setting is used for systems that have compact parameter space [30]. The other formulation is the *two-parameter semigroup* formulation, also called *process*, which is analogous to the general solutions of nonautonomous differential equations. Section 2.1 reviews these two formulations with some examples.

Since the time they have been introduced, attractors have been significantly important in terms of understanding the long run behaviour of dynamical systems. Although the first use of the term "attractor" was very early, in the 1950s, Milnor [50, 51] argued that until the mid of the 1980s there was no agreement on what is the most useful definition of attractors. Milnor proposes that a closed set A is called an *attractor* if: (i) it attracts a subset of the phase space with positive measure $\varrho(A)$, $\varrho(A)$ is called the *realm of attraction*; and (ii) it has no closed subset of $A' \subsetneqq A$ so that $\varrho(A')$ coincides with $\varrho(A)$ up to a set of measure zero. The first condition does not require the realm of attraction to be connected neighbourhood, whilst the second condition says that every part of the attractor has a role to play in the attraction.

Nonautonomous attractivity, especially the concept of pullback attractor has drawn a lot of attention in the last two decades by Kloeden, Cheban, Flandoli, Schmalfuß and others [31, 11, 10, 20]. Whilst forward attractors give an overview of the system in the long run (time tends to infinity), pullback attractors summarise what happens in the phase space at a certain time given that the system started in the distant past. This property of pullback attractors makes them useful tools for studying finite time transitions such as tipping points [4].

This chapter reviews basic concepts of nonautonomous systems theory. In Sections 2.1 and 2.2 we discuss the different formulation of NDSs as well as the limiting

behaviour and set-valued dynamics. Section 2.3 compares and contrasts two classes of nonautonomous systems, these are asymptotically autonomous systems and parameter shift systems. A discussion of nonautonomous attractivity is provided in Section 2.4.

2.1 Formulations of nonautonomous systems

There are two formulations for defining NDS t the skew product flows and the two-time parameter processes formulation. Skew product flow represents the nonautonomous dynamical system as autonomous systems over an extended phase space. It can be viewed as a solution of the following system of differential equations [30]:

$$\begin{aligned} \dot{y} &= f(y, \lambda), \\ \dot{\lambda} &= g(\lambda), \end{aligned} \tag{2.1}$$

where $y \in \mathbb{R}^n$, $\lambda \in \mathbb{R}^d$ and the functions $f : \mathbb{R}^n \times \mathbb{R}^d \to \mathbb{R}^n$ and $g : \mathbb{R}^d \to \mathbb{R}^d$ are sufficiently smooth. Note that $\dot{\lambda} = g(\lambda)$ is an autonomous system independent of y which can induce a flow $\lambda(t, \lambda_0) = \vartheta(t, \lambda_0)$, where λ_0 is an initial condition and $\vartheta : \mathbb{R} \times \mathbb{R}^d \to \mathbb{R}^d$ that satisfy $\vartheta(t + s, \lambda_0) = \vartheta(t, \vartheta(s, \lambda_0))$. We call $\vartheta(t, .)$ the *driving system* and $\mathbb{R}^d$ the *base space*.

The solution of $\dot{y} = f(y, \lambda)$ can be given as:

$$y(t, \lambda_0, y_0) := \phi(t, \lambda_0, y_0),$$

where $(\lambda_0, y_0) \in \mathbb{R}^d \times \mathbb{R}^n$ is an initial condition (i.e $\phi(0, \lambda_0, y_0) = y_0$) and ϕ is sufficiently smooth function $\phi : \mathbb{R} \times \mathbb{R}^d \times \mathbb{R}^n \to \mathbb{R}^n$ that satisfies:

(i) Initial condition property. $\phi(0, \lambda_0, y_0) = y_0$.

(ii) Cocycle property. $\phi(s + t, \lambda_0, y_0) = \phi(s, \vartheta(t, \lambda_0), \phi(t, \lambda_0, y_0))$.

Given that, the *skew product flow* of (2.1) is defined as $\pi : \mathbb{R} \times \mathbb{R}^d \times \mathbb{R}^n \to \mathbb{R}^d \times \mathbb{R}^n$

$$\pi(t, (\lambda, y)) := (\vartheta(t, \lambda), \phi(t, \lambda, y)).$$

for all $t \in \mathbb{R}$, $\lambda \in \mathbb{R}^d$ and $y \in \mathbb{R}^n$ [30, 58].

Example 2.1.1. Consider the following system of ordinary differential equations:

$$\begin{aligned} \dot{y} &= \lambda y, \\ \dot{\lambda} &= r. \end{aligned} \tag{2.2}$$

for some $r \neq 0$. Assuming that $x(0) = x_0$ and $\lambda(0) = \lambda_0$, then (2.2) has an explicit solution given by:

$$\begin{aligned} y(t) &= y_0 e^{t\lambda(t)} \\ \lambda(t) &= rt + \lambda_0. \end{aligned}$$

To put this in the aforementioned setting of skew product flow, we have $\vartheta : \mathbb{R}^2 \to \mathbb{R}$, $\vartheta(t, \lambda_0) := rt + \lambda_0$, $\phi : \mathbb{R}^2 \to \mathbb{R}, \phi(t, \lambda_0, y_0) := y_0 e^{t\theta(t,\lambda_0)}$; and finally the skew product flow $\pi : \mathbb{R}^3 \to R^2$ is defined as

$$\pi(t, (\lambda, y)) := (\vartheta(t, \lambda_0), \phi(t, \lambda_0, y_0)) = (rt + \lambda_0, y_0 e^{t(rt+\lambda_0)}).$$

The skew product formulation can be very useful for studying systems where the base space is compact [30]. The other formulation of NDSs is the two parameter processes, which is defined as the following [13].

Definition 2.1.1. A *process* Φ on $\mathbb{R}^n$ is a continuous function $\Phi : \mathbb{R} \times \mathbb{R} \times \mathbb{R}^n \to \mathbb{R}^n$ that satisfy the following conditions:

(i) $\Phi(s, s, x) = x$ for all $s \in \mathbb{R}$ and $x_0 \in \mathbb{R}^n$.

(ii) $\Phi(t, s, x) = \Phi(t, k, \Phi(k, s, x))$ for all $t, s, k \in \mathbb{R}$ and $x \in \mathbb{R}^n$.

The process formulation is analogous to the general solution of a nonautonomous ODE, as can be seen in the following example.

Example 2.1.2. Consider the following equation:

$$x = -2tx \tag{2.3}$$

that can be solved by separation of variables to give the following general solution:

$$x(t) = \Phi(t, s, x_s) = x_s e^{-(t^2 - t_0^2)}.$$

One can make sure that Φ satisfies the conditions of Definition 2.1.1 as the following:

- For any $s, x \in \mathbb{R}$ we have $\Phi(s, s, x) = xe^{-(s^2-s^2)} = xe^0 = x$.
- For any $t, s, k, x \in \mathbb{R}$ we have

$$\begin{aligned} \Phi(t, s, x) &= xe^{-(t^2-s^2)} = xe^{-(t^2-k^2+k^2-s^2)} = xe^{-(t^2-k^2)-(k^2-s^2)}, \\ &= xe^{-(k^2-s^2)}e^{-(t^2-k^2)} = \Phi(k, s, x)e^{-(t^2-k^2)} = \Phi(t, k, \Phi(k, s, x)). \end{aligned}$$

In the literature, the term *solution cocycle* is used to refer to the process induced by a nonautonomous differential equation. From now on, we may use both of these terms interchangeably. Furthermore, for simplification we use the two parameter process formulation to discus our results in Chapters 3 and 4 as well as to review the elements of NDSs theory in the rest of this chapter.

2.2 Nonautonomous invariance and limiting sets

In order to defined invariance, we consider the extended phase space $\mathbb{R} \times \mathbb{R}^n$ for a given process Φ on $\mathbb{R}^n$. We say $\mathcal{M} = \{M_t\}_{t\in\mathbb{R}}$ is a *nonautonomous set* if M_t is nonempty subset of $\mathbb{R}^n$ for all $t \in \mathbb{R}$. M_t is called the *t-fiber* of $\mathcal{M}$. Moreover, we say $\mathcal{M}$ has a property p, such as compactness, if M_t has p for all $t \in \mathbb{R}$.

We now define nonautonomous invariance.

Definition 2.2.1. Assume that $\mathcal{M} = \{M_t\}_{t\in\mathbb{R}}$ is a nonautonomous set of a dynamical system Φ we say $\mathcal{M}$ is Φ-*invariant* if it satisfies:

$$M_t = \Phi(t, s, M_s)$$

for all $t, s \in \mathbb{R}$.

For general nonautonomous systems, the forward and backward limits of nonautonomous sets can be at least as complex as an invariant set for an autonomous system (e.g. it may have a fractional dimension or indeed empty). However, under some conditions (see Section 2.3) these limits are well defined and quite useful for understanding the asymptotic behaviour of a system.

We use the upper limit of a sequence of sets [6] to define the limiting behaviour of a nonautonomous set $\mathcal{M}$. Note that, there is also a lower limit [6, 59], but the upper limit captures the asymptotic behaviour in a maximal sense.

Definition 2.2.2. Assume that $\mathcal{M} = \{M_t\}_{t\in\mathbb{R}}$ is a nonautonomous set of a nonautonomous dynamical system Φ. We define the *upper forward limit* $M_{+\infty}$ and the *upper backward limit* $M_{-\infty}$ for $\mathcal{M}$ as the following.

$$M_{+\infty} := \limsup_{t\to\infty} M_t = \bigcap_{\tau>0} \overline{\bigcup_{t\geq\tau} M_t},$$

$$M_{-\infty} := \limsup_{t\to-\infty} M_t = \bigcap_{\tau>0} \overline{\bigcup_{t\leq-\tau} M_t}.$$

We illustrate these concepts with examples.

Example 2.2.1. Consider Example 2.1.2 and system (2.3). The set $\mathcal{M} = \{M_t\}_{t\in\mathbb{R}}$ where $M_t = 0$ for any $t \in \mathbb{R}$ is Φ-invariant set with upper forward and upper backward limits $M_{+\infty} = M_{-\infty} = 0$.

Example 2.2.2. The dynamical system

$$\Phi(t, s, x_0) = x_0 e^{-(t-s)} + (t - s)e^{-t}$$

is induced by the following nonautonomous differential equation

$$\dot{x} = -x + e^{-t} \tag{2.4}$$

where $x, t, s \in \mathbb{R}$. Fixing $x_0 = s = 0$ the set $\mathcal{M} = \{\Phi(t, s, x_0)\}_{t\in\mathbb{R}} = te^{-t}$ is Φ-invariant set. Note that $M_{+\infty} = 0$ whilst $M_{-\infty}$ does not exist in $\mathbb{R}$.

In fact, any solution $x(t, s, x_0)$ for a autonomous differential equation $\dot{x} = f(t, x)$ where $t, s \in \mathbb{R}$ and $x, x_0 \in \mathbb{R}^n$ is an invariant set in the sense of Definition 2.2.1.

Note that for equation (2.4), $\lim_{t\to\infty} \Phi(t, s, x_0) = 0$ for any $s, x_0 \in \mathbb{R}$. However, the limit when $s \to -\infty$ is ∞. In autonomous systems there is no such confusion, as the system depends on the elapsed time $t - s$ and not on t or s explicitly. The difference between these two limits suggest that there are two ways of studying the asymptotic behaviour of a NDS: *forward limit* when $t \to \infty$, and *pullback limit* when $s \to \infty$. This is discussed in some detail in Section 2.4.

2.3 Two classes of nonautonomous systems

In this section, we present a class of nonautonomous systems that we use to understand rate-dependent phenomena, namely the parameter shift systems introduced in [4]. But first, we review more general class of NDSs so-called *asymptotically autonomous* systems [58, 74].

2.3.1 Asymptotically autonomous systems

A nonautonomous differential equation

$$\dot{x} = f(t, x), \tag{2.5}$$

where $f : \mathbb{R} \times \mathbb{R}^n \to \mathbb{R}^n$ is at least C^1 in both arguments, is called *past (future) asymptotically autonomous* with limiting equation

$$\dot{x} = g(x), \tag{2.6}$$

where $g : \mathbb{R}^n \to \mathbb{R}^n$ is at least C^1 too, if for any $x \in D$ the following limits hold uniformly [58]:

$$\lim_{t \to -\infty} f(t, x) = g(x),$$

for the past case, and for the future case we have:

$$\lim_{t \to \infty} f(t, x) = g(x).$$

We give an example of asymptotically autonomous system.

Example 2.3.1. Consider the modified form of equation (2.4) that is given by:

$$\dot{x} = -x + e^{at}. \tag{2.7}$$

It is past asymptotically autonomous to $\dot{x} = -x$ if $a < 0$ and future asymptotically autonomous to $\dot{x} = -x$ if $a > 0$.

Lemma 2.3.2 can be thought of a weaker version of [59, Lemma 5.1(1)], which states that the general solution of past asymptotically autonomous system behaves like the flow of its limit system, as time tends to $-\infty$. A similar statement can be made for future asymptotically autonomous systems.

Lemma 2.3.2. Assume that $\Phi : \mathbb{R} \times \mathbb{R} \times \mathbb{R}^n \to \mathbb{R}^n$ is the solution cocycle of (2.5) and $\phi : \mathbb{R} \times \mathbb{R}^n \to \mathbb{R}^n$ is the flow of (2.6). Then for any K compact and convex subset of $\mathbb{R}^n$ and any $\epsilon > 0$ and any $\tau > 0$ there is $\tau_0 < -\tau$ such that:

$$\|\Phi(s + t, s, x) - \phi(t, x)\| \leq \epsilon,$$

for all $s < \tau_0$, $0 \leq t \leq \tau$ and $x \in K$ with $\phi(t, x) \in K$.

Proof. The proof follows from [59, Lemma 5.1(1)]. □

The class of nonautonomous systems is useful for both modeling real-world phenomena and mathematically understanding their transitions. Ashwin *et al* [4] take this setting one step further to introduce parameter shift systems.

2.3.2 Parameter shift systems

Recall system (1.3),

$$\dot{x} = f(x, \Lambda(rt))$$

where $x \in \mathbb{R}^n$, $t, r \in \mathbb{R}$ and f is at least C^1 in both arguments. We fix $\lambda_- \leq \lambda_+$ and call the smooth function $\Lambda : \mathbb{R} \to \mathbb{R}$ a *parameter shift* [4] from λ_- to λ_+ if it varies between these limiting values, more precisely if it is a function $\Lambda : \mathbb{R} \to (\lambda_-, \lambda_+)$ such that:

(i) $\Lambda(\tau) \in [\lambda_-, \lambda_+]$, for all $\tau \in \mathbb{R}$;

(ii) $\lim_{\tau \to \pm\infty} \Lambda(\tau) = \lambda_\pm$;

(iii) $\lim_{\tau \to \pm\infty} d\Lambda/d\tau = 0$.

Figure 2.1 gives two examples of parameter shifts

The solution cocycle of (1.3) with $x(s) = x_0$ is denoted by the process

$$\Phi(t, s, x_0) := x(t).$$

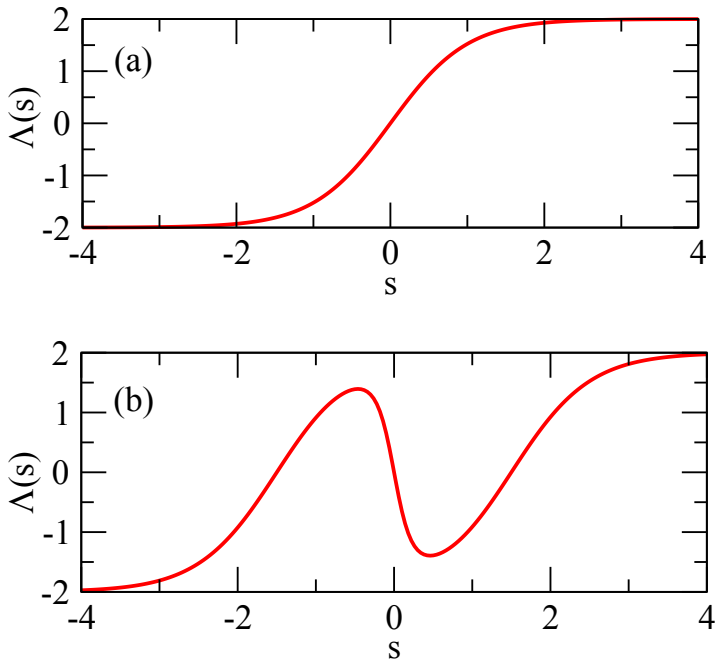

Figure 2.1: Two examples of parameter shifts. (a) is a monotonic, (b) nonmonotonic, shift from -2 to 2. The figure is taken from [4, Figure 1].

Note that Φ depends on r and Λ but we will suppress this dependence in most cases. There is an associated autonomous system for (1.3), which is given by (1.4), where λ is constant and denote the solution flow of (1.4) by $x(t, x_0) := \phi_\lambda(t, x_0)$. Also, there are two limiting systems, which are called *future (past) limit systems*

$$\dot{x} = f(x, \lambda_\pm) \tag{2.8}$$

with solution flow $x(t, x_0) := \phi_\pm(t, x)$. It is clear that (1.3) is future and past asymptotic to (2.8).

Example 2.3.3. Consider the following linear system.

$$\dot{x} = \Lambda x \tag{2.9}$$

where $x, t \in \mathbb{R}$ and $\Lambda(t) = \tanh(t)$. The future and past limit system of system (2.9)

are $\dot{x} = -x$ and $\dot{x} = x$ respectively. The solution cocycle can be given as:

$$\Phi(t, s, x_s) = \frac{x_s \cosh(t)}{\cosh(s)}.$$

The flows of the past and future limit systems can be given respectively as

$$\phi_-(t, x_0) = x_0 e^{-t}.$$

and

$$\phi_+(t, x_0) = x_0 e^{t}.$$

Similar to the case of (2.4), there are two approaches to define the limiting behaviour of Φ. Forward limiting behaviour, where $t \to \infty$, and pullback limiting behaviour, where $s \to -\infty$. It is obvious that system (2.9) is divergent in forward sense but converges to 0 in pullback sense. In such a case we say 0 is a pullback attractor for the system. Next section discusses nonautonomous attractivity in more detail.

2.4 Nonautonomous Attractivity

Following the discussion at the end of Section 2.3.2, there are different notions of attractivity for nonautonomous systems, depending on which time parameter is being fixed. The natural way to extend the classical (autonomous) concept of attractivity is by fixing the starting time s and considering the behaviour of the solutions when the actual time t tends to infinity, this is known as *forward attractivity*. On the other hand, *pullback attractivity* gives an overview of the behaviour of the system at finite actual time $t_0 \in \mathbb{R}$, when the starting time tends to $-\infty$.

Definition 2.4.1, after [30, Definition 3.3 and 3.4], present these different concepts. But first, we define Hausdorff semi-distance between two nonempty compact subsets X and Y of $\mathbb{R}^n$ by $d(X, Y) := \sup_{x \in X} \inf_{y \in Y} \|x - y\|$, the distance from a point x to

a set Y is given by $d(x,Y) := d(\{x\},Y)$, and the η-neighbourhood of M is defined

$$\mathcal{N}_\eta(M) := \{x \in \mathbb{R}^n \ : \ d(x,M) < \eta\}.$$

The Hausdorff distance[30] between two nonempty compact subsets X and Y of $\mathbb{R}^n$ is defined

$$d_H(X,Y) := \max\{d(X,Y), d(Y,X)\}.$$

Definition 2.4.1. Let Φ be a process. A compact and Φ-invariant nonautonomous set $\mathcal{A}$ is said to be:

(i) *a global forward attractor* if for any bounded set $B \subset \mathbb{R}^n$,

$$\lim_{t\to\infty} d(\Phi(t,s,B), A_t) = 0 \qquad \text{for all } s \in \mathbb{R}.$$

(ii) a global pullback attractor if for any bounded set $B \subset \mathbb{R}^n$,

$$\lim_{s\to-\infty} d(\Phi(t,s,B), A_s) = 0 \qquad \text{for all } t \in \mathbb{R}.$$

We illustrate these different concepts of attractivity in the following example.

Example 2.4.1. Consider the following modified version of equation 2.2.

$$\dot{x} = 2atx \tag{2.10}$$

with the solution cocycle $\Phi(t,s,x_s) = x_s e^{a(t^2-s^2)}$. Now consider the nonautonomous set $\mathcal{A} = \{A_t\}_{t\in\mathbb{R}}$ with t-fibers $A_t = \{0\}$ for all $t \in \mathbb{R}$. $\mathcal{A}$ is a global pullback attractor if $a > 0$ and a forward attractor if $a < 0$.

Example 2.4.1 shows that the concepts of pullback and forward attractivity are independent. However, that is not the case in autonomous systems. So far, we

have discussed and reviewed the attractivity of NDS in a global sense. Nevertheless, critical transitions take place in multi-stable systems where the attractors are local. Chapter 3 reviews the concept of local pullback attractor and its role in understanding R-tipping.

Chapter 3

Local pullback attractors and tipping

Whilst global pullback attractors attract all bounded subsets of the phase space in pullback sense, local pullback attractors act on a specific neighbourhood in the phase space. Whether that neighbourhood should be a nonautonomous set that contains the pullback attractor (time-dependent) or an autonomous open set that contains the upper backward limit of the pullback attractor, is a matter of disagreement. Kloeden and Rasmussen [30, Definition 3.48] define local pullback attractor $\mathcal{A} = \{A_t\}_{t\in\mathbb{R}}$ as Φ-invariant compact nonautonomous set that attracts time-dependent neighbourhood in pullback sense. Ashwin et al [4, Definition 2.3], on the other hand, require the neighbourhood to contain the upper backward limit of $\mathcal{A}$ and not necessarily the entire attractor[1]. For general nonautonomous systems we show that Kloeden and Rasmussen's definition is more general than the definition given in Ashwin *et al* [4], see Proposition 3.1.1 and Example 3.1.2.

Pullback attracting solutions, has been shown as a useful tool to study rate-induced tipping from equilibria [4], In particular, it has been shown that for param-

[1]Definition 2.3 in [4] defines pullback attracting solutions for parameter shift system where the upper backward limit is the same as the lower one. However, extending the definition for general pullback attractors requires one to consider the upper backward limits, see Section 3.1 for more details.

eter shift systems (1.3) if there is an exponentially stable equilibrium X_- for the past limit system, then there is a pullback attracting solution $\tilde{x}_t^{[\Lambda,r,X_-]}$ that limits backward in time to X_-, and depends on r and Λ. Moreover, [4] proposed that R-tipping is associated with changes in the properties of $\tilde{x}_t^{[\Lambda,r,X_-]}$. Namely, R-tipping occurs if there is a positive value of r at which $\tilde{x}_t^{[\Lambda,r,X_-]}$ limits to a repeller of the future limit system. A detailed review of these results is given in Section 3.2.

3.1 Properties of local pullback attractors

This section compares two different definitions of local pullback attractors, these are Kloeden and Rasmussen's [30, Definition 3.48] and Ashwin *et al* [4, Definition 2.3].

We define local pullback attractor similar to [30, Definition 3.48].

Definition 3.1.1. Suppose that Φ is a process on $\mathbb{R}^n$. A compact and Φ-invariant nonautonomous set $\mathcal{A}$ is called *local pullback attractor* if there exists an $\eta > 0$ such that for all $t \in \mathbb{R}$

$$\lim_{s\to-\infty} d(\Phi(t,s,\mathcal{N}_\eta(A_s)),A_t) = 0,$$

where d is Hausdorff semi-distance and $\mathcal{N}_\eta(A_s)$ the η-neighbourhood of A_s.

Definition 3.1.1 requires the pullback attractor to attract a nonautonomous neighbourhood (time-dependent) $\{\mathcal{N}_\eta(A_t)\}_{t\in\mathbb{R}}$ in pullback sense. However, if the upper backward limit of $\mathcal{A}$ is bounded, we argue that one can consider an autonomous neighbourhood (time-independent) of the upper backward limit of $\mathcal{A}$, which is equivalent to [4, Definition 2.3].

Lemma 3.1.1. Suppose that Φ is a process, $\mathcal{A}$ is a compact nonautonomous Φ-invariant set with upper backward limit $A_{-\infty}$. Then $\mathcal{A}$ is a pullback attractor if there is a bounded open set U containing $A_{-\infty}$ that satisfy

$$\lim_{s\to-\infty} d\left(\Phi(t,s,U),A_t\right) = 0 \tag{3.1}$$

for all $t \in \mathbb{R}$.

Proof. Assume that there is a bounded open set $U \subset \mathbb{R}^n$ that contains $A_{-\infty}$ such that (3.1) is satisfied for all $t \in \mathbb{R}$. We need to prove that $\mathcal{A}$ is a pullback attractor.

Note that, as $A_{-\infty}$ is the upper backward limit of $\mathcal{A}$, then for any $s_0 < 0$ there is an $\eta > 0$ such that $A_s \subset \mathcal{N}_\eta(A_{-\infty})$ for all $s < s_0$. Now choose s_0 small enough such that $\mathcal{N}_\eta(A_{-\infty}) \subset U$, we have

$$\Phi(t, s, \mathcal{N}_\eta(A_s)) \subset \Phi(t, s, U)$$

for all $s < s_0$, which means:

$$\lim_{s \to -\infty} d(\Phi(t, s, \mathcal{N}_\eta(A_s)), \Phi(t, s, U)) = 0.$$

But we already have that $\lim_{s\to-\infty}(\Phi(t, s, U), A_t) = 0$ from (3.1). Thus, by the triangle inequality of Hausdorff semi-distance we have:

$$\lim_{s \to -\infty}(\Phi(t, s, \mathcal{N}_\eta(A_s)), A_t) = 0,$$

and $\mathcal{A}$ is pullback attractor according to Definition 3.1.1. □

Ashwin *et al* [4] have pointed out that their definition of local pullback attractor is different than Definition 3.1.1. However, Proposition 3.1.1 shows that a pullback attractor with respect to [4, Definition 2.3] is necessarily a pullback attractor with respect to Definition 3.1.1. Example 3.1.2 shows that the other direction is not true in general. However, it might be provable with some extra assumptions such as Φ is induced by an asymptotically autonomous system of ODEs, and the upper backward limit of $\mathcal{A}$ is the same as the lower backward limit.

Example 3.1.2. We give an example of a system that has local pullback attractors in the sense of definition 3.1.1, but there is no neighbourhood $\mathcal{N}_\eta(A_{-\infty})$ of the upper

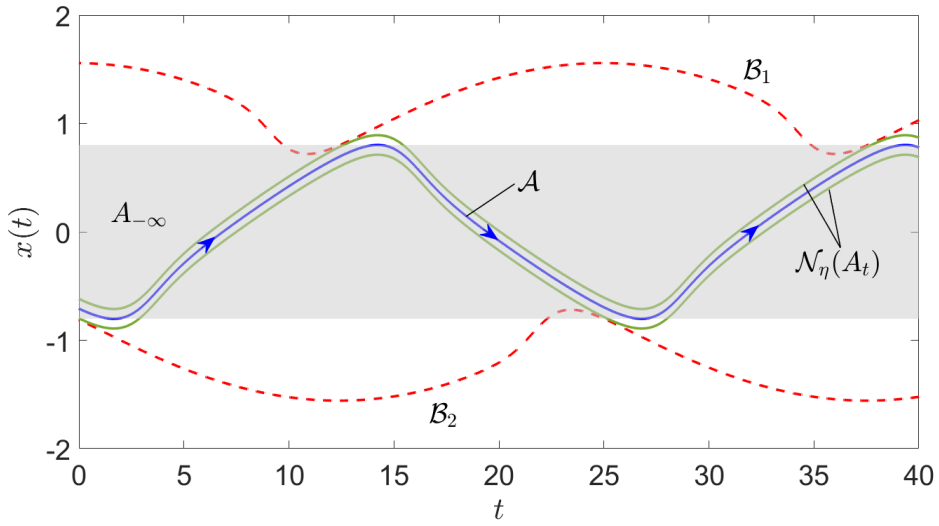

Figure 3.1: The time profile of system 3.2. It shows the uniform attractor $\mathcal{A}$, the blue solid curve, and the repellers $\mathcal{B}_{1,2}$, the red dashed curves. The two green curves represent the boundaries of the neighbourhood $\mathcal{N}_\eta(A_t)$,where $0 \leq \eta \leq 0.09$. It can be seen that $\mathcal{N}_\eta(A_t)$ lies entirely between $\mathcal{B}_1$ and $\mathcal{B}_2$ which means it is uniformly attracted to $\mathcal{A}$, which means that $\mathcal{A}$ is a local pullback attractor in the sense of definition 3.1.1. The gray region is the upper backward limit $A_{-\infty} \approx [-0.8, 0.8]$. It can be seen that it intersects $\mathcal{B}_{1,2}$, i.e any neighbourhood of $\mathcal{N}_\eta(A_{-\infty})$ can not be attracted to $\mathcal{A}$ in pullback sense. The parameter values are $\alpha = 1.784$, $\beta = 1$ and $\omega = 0.25$.

backward limit $A_{-\infty}$ that satisfy

$$\lim_{s \to -\infty} d\left(\Phi(t, s, \mathcal{N}_\eta(A_{-\infty})), A_t\right) = 0.$$

Consider the following ordinary differential equation:

$$\dot{x} = -\alpha x + x^3 - \beta \cos(\omega t). \tag{3.2}$$

For $\beta = 0$ and $\alpha > 0$ the system is autonomous with three equilibria $x = 0$ which is stable and $x = \pm\sqrt{\alpha}$ which are unstable. The nonautonomous system, however, has no equilibria. Instead, it has three invariant curves: $\mathcal{A}$ which is uniform local attractor and $\mathcal{B}_{1,2}$ which are uniform repellers. We compute these three curves for specific parameter values ($\alpha = 1.784$, $\beta = 1$ and $\omega = 0.25$). Figure 3.1 shows that $\mathcal{A}$ locally attracts small neighbourhood $\mathcal{N}_\eta(A_t)$ for any $\eta \in (0, 0.09]$. Furthermore, it

shows that the upper backward limit $A_{-\infty}$, which is in this case given by the interval $[-0.8, 0.8]$, intersects $\mathcal{B}_{1,2}$. This means, for any $\eta > 0$ the neighbourhood $\mathcal{N}_\eta(A_{-\infty})$ can not be entirely attracted by $\mathcal{A}$ in pullback sense.

3.2 Pullback attractors for parameter shift systems

In this section, we review some results from [4] that are related to pullback attracting solutions. We extend these results in Chapter 4 to be applicable for a larger class of attractors. As in [4], we denote the set of all equilibria for the bifurcation diagram of (1.4) by $\mathcal{X} = \{(X, \lambda) \in \mathbb{R}^{n+1} : f(X, \lambda) = 0\}$. The subset of all linearly stable equilibria is denoted by $\mathcal{X}_{\text{stab}} \subset \mathcal{X}$.

The first theorem we introduce is [4, Theorem 2.2] that shows for any exponentially stable equilibria X_- of the past limit system (2.8), there is a pullback attracting solution $\tilde{x}_{pb}^{[\Lambda,r,X_-]}(t)$ of the nonautonomous system (1.3). And this pullback attractor limits to X_- backward in time.

Theorem 3.2.1. [4, Theorem 2.2] Suppose that $(X_-, \lambda_-) \in \mathcal{X}_{\text{stab}}$, there is a pullback attractor $\tilde{x}_{pb}^{[\Lambda,r,X_-]}(t)$ of (1.3) which limits to X_- backward in time.

Note that, the pullback attractor $\tilde{x}_{pb}^{[\Lambda,r,X_-]}(t)$ is uniquely determined by Λ, r and X_-. A smooth curve $X(\lambda)$ in $\overline{\mathcal{X}_{\text{stab}}}$,$\lambda \in (\lambda_-, \lambda_+)$, is called a *stable branch* for (1.4). Moreover, given two equilibria X_- and X_+ with $(X_\pm, \lambda_\pm) \in \mathcal{X}$, we say they are Λ-*connected* if there is a stable branch between $X(\lambda)$ that limit to them as $\lambda \to \lambda_\pm$. As mentioned in Section 1.2 $X(\lambda)$ represent the QSA of (1.3), assuming that $(X_\pm, \lambda_\pm) \in \mathcal{X}_{\text{stab}}$ are Λ-connected with the stable branch $X(\lambda)$. The following result [4, Lemma 2.3] shows that such a QSA can give a valid approximation of the pullback attractor $\tilde{x}_{pb}^{[\Lambda,r,X_-]}(t)$, for a range of small values of $r > 0$.

Lemma 3.2.2. [4, Lemma 2.3] Suppose that $(X_\pm, \lambda_\pm) \in \mathcal{X}_{stab}$ are Λ-connected with

a stable branch $X(\Lambda(\tau))$. Then for any $\delta > 0$ there exists $r_c > 0$ such that

$$\left\| \tilde{x}_{pb}^{[\Lambda,r,X_-]}(t) - X(rt) \right\| < \delta,$$

for all $0 < r < r_c$. Moreover, $\lim_{t\to\infty} \tilde{x}_{pb}^{[\Lambda,r,X_-]}(t) = X_+$ for all sufficiently small $r > 0$.

In other words, Lemma 3.2.2 shows that for a range of small enough positive r the pullback attractor $\tilde{x}_{pb}^{[\Lambda,r,X_-]}(t)$ *tracks* the QSA of the system, but that is not necessarily true for large r. Rate-dependent tipping occurs when such a tracking is no longer tacking place, as the following definition [4, Definition 3.2] explains.

Definition 3.2.1. [4, Definition 3.2] Let $X_-(\lambda)$ be a stable branch of equilibria that are linearly stable for all $\lambda \in [\lambda_-, \lambda_+]$, Consider $X_\pm = X(\lambda_\pm)$ and the pullback attractor $\tilde{x}_{pb}^{[\Lambda,r,X_-]}(t)$ that limits backward in time to X_-. We say there is *R-tipping* if there exists $r_c > 0$ such that:

$$\lim_{t\to\infty} \tilde{x}_{pb}^{[\Lambda,r,X_-]}(t) \begin{cases} = X_+ & \text{for } 0 < r < r_c \\ \neq X_+ & \text{for } r = r_c \end{cases}$$

Theorem 3.2.1, Lemma 3.2.2 and Definition 3.2.1 provide a scenario for the occurrence of R-tipping under the setting of parameter shift systems. Example 1.2.1 illustrates similar scenario, although the forcing in (1.5) is not parameter shift. In the following example we analyse (1.5) with parameter shift forcing.

Example 3.2.3. We consider the normal form of fold bifurcation once again, but this time with parameter shift forcing:

$$\begin{aligned} \dot{x} &= (x + \Lambda(rt))^2 - \mu \\ \dot{\Lambda} &= r\Lambda(\lambda_{\max} - \Lambda) \end{aligned} \tag{3.3}$$

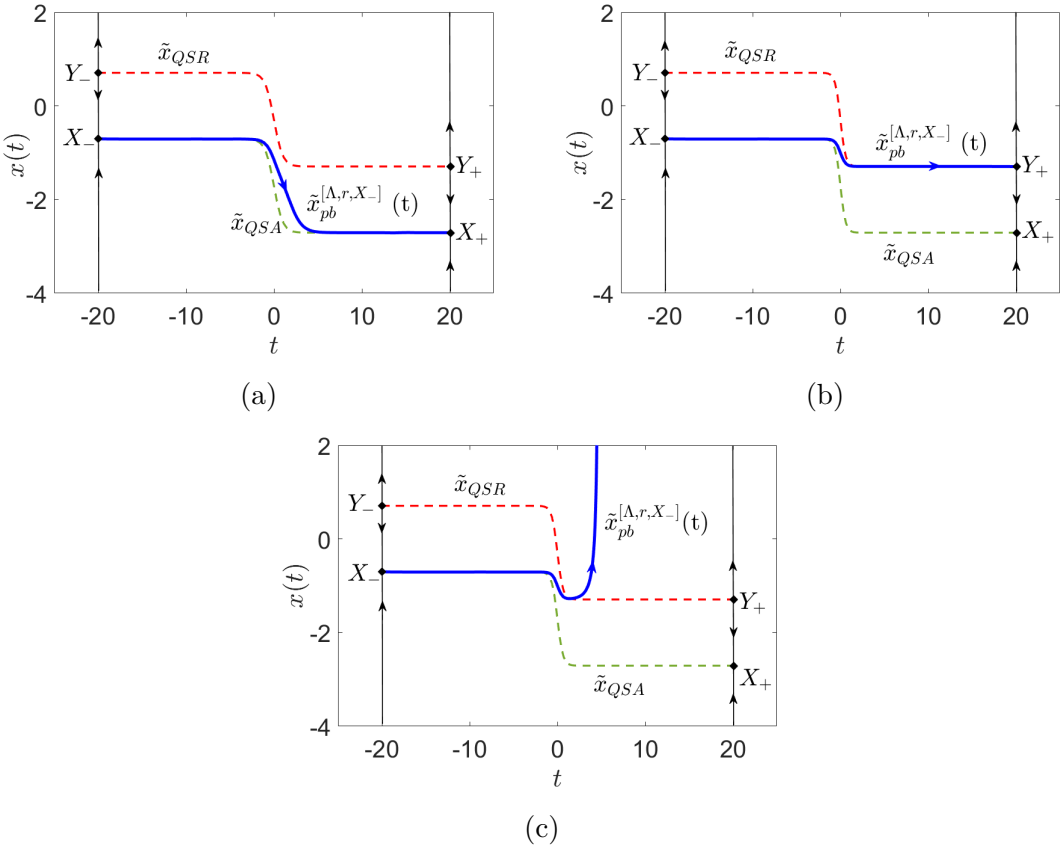

Figure 3.2: The different types of behaviour of (3.3) with respect to different values of the parameter r, (a) the tracking case $r < r_c$ (b) the tipping case where $r = r_c$ and (c) shows that the pullback attractor blow up to infinity as $r > r_c$. The parameter values are $\mu = 0.5$ and $\lambda_{\max} = 2$.

with $x(t), \Lambda(rt) \in \mathbb{R}$ and $r > 0$. The parameter shift Λ is illustrated in Figure 1.4 for $r = 1$ and $\lambda_{\max} = 8$.

The past limit system $\dot{x} = x^2 - \mu$ has two equilibria, $X_- = -\sqrt{\mu}$ is stable, and $Y_- = \sqrt{\mu}$ is unstable. Whilst the future limit system has $X_+ = -\sqrt{\mu} - \lambda_{\max}$ as stable equilibrium and $Y_+ = \sqrt{\mu} - \lambda_{\max}$ as unstable one.

The QSA of the system is given by $\tilde{x}_{\mathrm{QSA}}(t) = -\sqrt{\mu} - \Lambda(rt)$. Also, there is a quasi-static repeller for the that given by $\tilde{x}_{\mathrm{QSR}}(t) = \sqrt{\mu} - \Lambda(rt)$. One can approximate the pullback attractor $\tilde{x}_{pb}^{[\Lambda,r,X_-]}$ numerically by solving (3.3) for close enough initial condition to X_-. According to Lemma 3.2.2, $\tilde{x}_{pb}^{[\Lambda,r,X_-]}(t)$ tracks $\tilde{x}_{\mathrm{QSA}}(t)$, for small enough $r > 0$.

Perryman [57] has shown that there is a critical rate for this system, which can

be given by:

$$r_c = \frac{2\mu\lambda_{\max}}{2(\lambda_{\max} - 2\sqrt{\mu})},$$

and at this rate there is a heteroclinic connection between X_- and Y_+. In other words, the pullback attractor $\tilde{x}_{pb}^{[\Lambda, r_c, X_-]}(t) \to Y_+$ as $t \to \infty$, Which means the systems undergo R-tipping at $r = r_c$ according to definition 3.2.1. Figure 3.2 illustrate the behaviour of (3.3) for different values of $r > 0$.

This tracking-tipping scenario is not restricted to systems that have only equilibrium attractors. As Chapter 4 shows, it can be generalised to include any compact exponentially stable attractors. Nevertheless, as the complexity of attractors increases, more interesting rate-dependent phenomena, such as partial tipping and weak tracking, may occur.

Chapter 4

Parameter shift systems with non-equilibrium attractors

Due to the comparability with the associated autonomous systems (1.4), parameter shift systems (1.3) are very useful for studying critical transitions and tipping points [4]. This chapter assumes that the attractors of the limit systems are compact and exponentially stable. In contrast to [4], we do not require our limiting attractors to be equilibria neither the system to be one dimensional.

We prove in Theorem 4.2.2 that any asymptotically stable attractor for the past limit system is associated with a pullback attractor for the parameter shift system. This pullback attractor tracks a branch of exponentially stable attractors for the associated autonomous systems, for a range of small rate, see Theorem 4.3.1. Rate-induced transitions take place when this tracking is violated at some critical rate r_c. Definition 4.3.1 defines four different rate-induced phenomena these are: weak tracking, strong tracking, partial tipping, and total tipping.

The main results of this chapter have been published in *Chaos: An Interdisciplinary Journal of Nonlinear Science* [1, Sections II and III].

4.1 Bifurcations of the autonomous system

Recall that Φ is the solution cocycle of (1.3), ϕ_λ is the flow induced by (1.4) and $\phi_\pm$ are the flows of the future and past limit systems. A compact ϕ_λ-invariant subset $M \subset \mathbb{R}^n$ is called *Lyapunov stable* if for all $\epsilon > 0$ there exists a $\delta > 0$ such that

$$d(\phi_\lambda(t, y), M) < \epsilon \text{ for all } t > 0 \text{ for all } y \in \mathcal{N}_\delta(M).$$

A Lyapunov stable compact invariant set M is called *asymptotically stable* if there exists an $\eta > 0$ such that:

$$\lim_{t\to\infty} d(\phi_\lambda(t, y), M) = 0 \text{ for all } y \in \mathcal{N}_\eta(M),$$

[23, Definition 5.34] defines exponential stability for equilibria in global sense, and the following definition extends this concept to general compact attractors in local sense.

Definition 4.1.1. We say a connected compact invariant set $M \subset \mathbb{R}^n$ is *exponentially stable* for ϕ_λ if there are $\mu > 0$, $\eta > 0$ and $C \geq 1$ such that

$$d(\phi_\lambda(t, x), M) \leq Ce^{-\mu t} d(x, M) \tag{4.1}$$

for all $x \in \mathcal{N}_\eta(M),\ t > 0$.

Note that this implies that M is asymptotically stable. In Section 3.2 we denote the set of all equilibria of (1.4) by $\mathcal{X}$, here we extend it to include all compact and connected invariant sets. The subset of all exponentially stable compact invariant sets is denoted by $\mathcal{X}_{\text{stab}} \subset \mathcal{X}$, this includes attracting equilibria and periodic orbits. Moreover, we call $\overline{\mathcal{X}_{\text{stab}}} \setminus \mathcal{X}_{\text{stab}}$ the set of bifurcation points.

Analogous to [4, definitions 2.1 and 2.2] we define *stable path* and *stable branch* of compact attractors as the following.

Definition 4.1.2. A continuous set valued function $A(\lambda) \in \mathcal{X}_{\text{stab}}$ that limits to some $(A_\pm, \lambda_\pm) \in \mathcal{X}$ is called a *stable path*.

If the choices μ, η, C in (4.1) can be made uniformly (independent of λ) on a stable path then we say the path is *uniformly stable*.

Definition 4.1.3. We say a smooth curve $A(\lambda)$ is *stable branch* if $A(\lambda)$ is uniformly exponentially stable for all $\lambda \in (\lambda_1, \lambda_2)$, where $\lambda_- \leq \lambda_1 \leq \lambda_2 \leq \lambda_+$.

The example in Chapter 5 only has branches of attractors of (1.4) that are periodic orbits but, unless indicated, the remaining results hold for branches of more general attractors.

4.2 Local pullback attractors and their limiting behaviour

This section examines the existence of pullback attractors for parameter shift systems, and how related they are to the attractors of the past limit system. Moreover, we study in this section some properties of forward and backward limits of Φ-invariant sets.

4.2.1 The invariance of backward/forward limiting sets

The following result shows that for a particular Φ-invariant set $\mathcal{A}$, the backward limit $A_{-\infty}$ (forward limit $A_{+\infty}$) is invariant for the corresponding limit systems.

Lemma 4.2.1. For a parameter shift from λ_- to λ_+ and a nonautonomous invariant set $\mathcal{A}$ with fibre A_t, if $A_{\pm\infty}$ is bounded then we have

$$\phi_\pm(t, A_{\pm\infty}) = A_{\pm\infty}$$

for all $t \in \mathbb{R}^+$.

Proof. We prove in detail for the past limit case: the future limit proof follows similarly.

We pick a sufficiently large compact and convex set K that contain $A_{-\infty}$. From the definition of $A_{-\infty}$, there exists $\tau_1 < 0$ such that $A_s \subset K$ for all $s < \tau_1$. Moreover, using Lemma 2.3.2 we have for all $\tau > 0$ and $\epsilon > 0$ there exists $\tau_2 < -\tau$ such that

$$d_H\left(\Phi(s+t, s, A_{-\infty}), \phi_-(t, A_{-\infty})\right) < \epsilon/3$$

for all $s < \tau_2$ and $t \in [0, \tau]$. Define $\tau_0 := \min\{\tau_1, \tau_2\}$, we have

$$d_H\left(\Phi(s, s-t, A_{s-t}), \phi_-(t, A_{s-t})\right) < \epsilon/3$$

for all $s < \tau_0$ and $t \in [0, \tau]$. But $\mathcal{A}$ is Φ-invariant, meaning $\Phi(s, s-t, A_{s-t}) = A_s$. Therefore,

$$d_H\left(A_s, \phi_-(t, A_{s-t})\right) < \epsilon/3.$$

For simplification we define $B_u := \overline{\cup_{t<u} A_t}$. Note that $d_H(B_u, A_{-\infty}) \to 0$ as $u \to -\infty$, i.e. for all $\epsilon > 0$ there is $u_0 < 0$ such that $d_H(B_u, A_{-\infty}) < \epsilon/3$ for all $u \leq u_0$. Also,

$$\begin{aligned} d_H\left(B_{\tau_0}, \phi_-(t, B_{\tau_0 - t})\right) &\leq d_H\left(\overline{\cup_{s<\tau_0} A_s}, \phi(t, \overline{\cup_{s<\tau_0 - t} A_s})\right) \\ &\leq \sup_{s<\tau_0}\{d_H(A_t, \phi_-(t, A_{s-t}))\} < \epsilon/3. \end{aligned}$$

Note that since ϕ_- is a diffeomorphism then there is a Lipschitz constant C such that for any fixed $t \in \mathbb{R}$ and any $D \subset \mathbb{R}^n$ we have $d_H\left(\phi_-(t, D), \phi_-(t, A_{-\infty})\right) \leq C d_H\left(D, A_{-\infty}\right)$. Now choose $v_0 < 0$ such that for all $v < v_0$ we have $d_H(B_v, A_{-\infty}) < \epsilon/3C$. Therefore,

$$d(\phi_-(t, B_v), A_{t, A_{-\infty}}) \leq C d_H(B_v, A_{-\infty}) < C\epsilon/3C = \epsilon/3.$$

Now choose $\nu = \min\{\tau_0, u_0, v_0\}$ and use the triangle inequality, we have for any $\epsilon > 0$

$$\begin{aligned} d_H\left(A_{-\infty}, \phi_-(t, A_{-\infty})\right) &\leq d_H\left(A_{-\infty}, B_\nu\right) + d_H\left(B_\nu, \phi_-(t, B_{\nu-t})\right) \\ &+ d_H\left(\phi_-(t, B_{\nu-t}), \phi_-(t, A_{-\infty})\right) \\ &< \epsilon/3 + \epsilon/3 + \epsilon/3 = \epsilon. \end{aligned}$$

□

4.2.2 The existence of local pullback attractors

The following result generalises Theorem 3.2.1, as it gives a sufficient condition that there is a local pullback attractor whose backward limit is contained within an attractor of the past limit system.

Theorem 4.2.2. Suppose that A_- is an asymptotically stable attractor for the past limit system ϕ_-. Then there is local pullback attractor of Φ whose (upper) backward limit is contained in A_-.

We delay the proof of Theorem 4.2.2 to give two lemmas that will be used in the proof.

Lemma 4.2.3. Assume that A_- is an asymptotically stable attractor for the past limit system ϕ_-. Then there is $\tilde{\eta} > 0$ such that for all $\eta \in (0, \tilde{\eta}]$ and all $\delta > 0$ there exist $\tau > 0$ and $\tilde{\tau} > 0$ such that $\Phi(t, s, \mathcal{N}_\eta(A_-)) \subset \mathcal{N}_\delta(A_-)$, for all t and s such that $s < t - \tilde{\tau}$ and $t < -\tau$.

Proof. Asymptotic stability of A_- means that there is a $\tilde{\eta} > 0$ such that for any $0 < \eta < \tilde{\eta}$ we have

$$\lim_{s \to \infty} d(\phi_-(s, \mathcal{N}_\eta(A_-)), A_-) = 0.$$

This means that for any $\delta > 0$ there is $\tilde{\tau} > 0$ such that $d(\phi_-(k, \mathcal{N}_\eta(A_-)), A_-) < \delta/2$

for all $k > \tilde{\tau}$. By [59, Lemma 5.1], for any $\delta > 0$ and $k > \tilde{\tau}$ there is $\tau > 0$ such that

$$d_H(\Phi(u, u-k, \mathcal{N}_\eta(A_-)), \phi_-(k, \mathcal{N}_\eta(A_-))) < \delta/2$$

for all $u < -\tau$. The triangle inequality of Hausdorff semi-distance implies

$$\begin{aligned} d\left(\Phi(u, u-k, \mathcal{N}_\eta(A_-)), A_-\right) &\leq d\left(\Phi(u, u-k, \mathcal{N}_\eta(A_-)), \phi_-(k, \mathcal{N}_\eta(A_-))\right) \\ &+ d\left(\phi_-(k, \mathcal{N}_\eta(A_-), A_-\right) \\ &< \delta/2 + \delta/2 = \delta. \end{aligned}$$

for all u and k such that $u < -\tau$ and $u - k < u - \tilde{\tau}$, which completes the proof. □

For $\tilde{\eta}$ as in Lemma 4.2.3 and $\eta \in (0, \tilde{\eta}]$, we define $\mathcal{A}^{[\Lambda, r, A_-]} := \left\{A_t^{[\Lambda, r, A_-]}\right\}_{t \in \mathbb{R}}$ where:

$$A_t^{[\Lambda, r, A_-]} := \bigcap_{\tau > 0} \overline{\bigcup_{s \leq -\tau} \Phi\left(t, s, \mathcal{N}_\eta(A_-)\right)} \tag{4.2}$$

for all $t \in \mathbb{R}$ (recall that Φ is the solution of (1.3) and so depends on r and Λ).

Lemma 4.2.4. Assume that A_- is asymptotically stable attractor for the past limit system ϕ_-. Then the nonautonomous set (4.2) is independent of η for all $\eta \in (0, \tilde{\eta}]$.

Proof. Consider any η and η' in $(0, \tilde{\eta}]$, assume $\eta' < \eta$ *w.l.o.g* and define

$$\begin{aligned} A_t &= \bigcap_{\tau > 0} \overline{\bigcup_{s \leq -\tau} \Phi\left(t, s, \mathcal{N}_\eta(A_-)\right)}, \\ A'_t &= \bigcap_{\tau > 0} \overline{\bigcup_{s \leq -\tau} \Phi\left(t, s, \mathcal{N}_{\eta'}(A_-)\right)}. \end{aligned}$$

Since $\mathcal{N}_{\eta'}(A_-) \subset \mathcal{N}_\eta(A_-)$ we have

$$\bigcap_{\tau > 0} \overline{\bigcup_{s \leq -\tau} \Phi\left(t, s, \mathcal{N}_{\eta'}(A_-)\right)} \subset \bigcap_{\tau > 0} \overline{\bigcup_{s \leq -\tau} \Phi\left(t, s, \mathcal{N}_\eta(A_-)\right)}$$

which means $A'_t \subset A_t$. We also have to show that $A_t \subset A'_t$. By Lemma 4.2.3 there exist τ, $\tilde{\tau} > 0$, such that $\Phi(k, s, \mathcal{N}_\eta(A_-)) \subset \mathcal{N}_{\eta'}(A_-)$, for all $s < k - \tilde{\tau}$ and $k < -\tau$.

Now, for all $t \in \mathbb{R}$

$$\begin{aligned}
\Phi\left(t, k, \Phi\left(k, s, \mathcal{N}_\eta(A_-)\right)\right) &\subset \Phi\left(t, k, \mathcal{N}_{\eta'}(A_-)\right), \\
\Phi\left(t, s, \mathcal{N}_\eta(A_-)\right) &\subset \Phi\left(t, k, \mathcal{N}_{\eta'}(A_-)\right), \\
\bigcap_{\tau>0} \overline{\bigcup_{s<-\tau-\tilde{\tau}} \Phi\left(t, s, \mathcal{N}_\eta(A_-)\right)} &\subset \bigcap_{\tau>0} \overline{\bigcup_{k<-\tau} \Phi\left(t, k, \mathcal{N}_{\eta'}(A_-)\right)}, \\
A_t &\subset A'_t.
\end{aligned}$$

Therefore $A_t = A'_t$ for all $t \in \mathbb{R}$ and so $\mathcal{A}^{[\Lambda, r, A_-]}$ is independent of choice of $\eta \in (0, \tilde{\eta}]$. □

Proof. (For Theorem 4.2.2)

To show that $A_{-\infty}^{[\Lambda, r, A_-]} \subset A_-$, choose $\tilde{\eta}$ as in Lemma 4.2.3, and pick any $\eta \in (0, \tilde{\eta}]$. By Lemma 4.2.4, the upper backward limit of $\mathcal{A}^{[\Lambda, r, A_-]}$ can be uniquely defined as:

$$A_{-\infty}^{[\Lambda, r, A_-]} = \bigcap_{\tau>0} \overline{\bigcup_{t \le -\tau} A_t^{[\Lambda, r, A_-]}} = \bigcap_{\tau>0} \overline{\bigcup_{\substack{t \le -\tau \\ s<t}} \Phi\left(t, s, \mathcal{N}_\eta(A_-)\right)}.$$

By Lemma 4.2.3, for all $\delta > 0$ there exists $\tau, \tilde{\tau} > 0$ such that

$$\bigcup_{\substack{t \le -\tau \\ s<t-\tilde{\tau}}} \Phi(t, s, \mathcal{N}_\eta(A_-)) \subset \mathcal{N}_\delta(A_-)$$

which gives

$$A_{-\infty}^{[\Lambda, r, A_-]} = \bigcap_{\tau>0} \overline{\bigcup_{\substack{t \le -\tau \\ s<t}} A_t^{[\Lambda, r, A_-]}} \subset \mathcal{N}_\delta(A_-).$$

Recall this holds for all $\delta > 0$, which in turn implies that $A_{-\infty}^{[\Lambda, r, A_-]} \subset \overline{A_-} = A_-$.

To show that (4.2) is a pullback attractor, we need to show it is compact, invariant and attracts a neighbourhood. For all $t \in \mathbb{R}$, $A_t^{[\Lambda, r, A_-]}$ is intersection of closed sets, which implies that it is closed. To show that it is compact, we just need to

show it is bounded. By using Lemma 4.2.3 again, $\Phi(s_2, s_1, \mathcal{N}_\eta(A_-)) \subset \mathcal{N}_\eta(A_-)$ for all $s_1 < s_2 - \tilde{\tau} < -\tau$, by the cocycle property of Φ we get:

$$\bigcup_{s<-\tau} \Phi(t, s, \mathcal{N}_\eta(A_-)) \subset \Phi(t, -\tau, \mathcal{N}_\eta(A_-)).$$

Now since $\Phi(t, s, .)$ is a diffeomorphism for all $t, s \in \mathbb{R}$, $\Phi(t, -\tau, \mathcal{N}_\eta(A_-))$ is bounded, and so $\bigcup_{s<-\tau} \Phi(t, s, \mathcal{N}_\eta(A_-))$ is bounded. Hence, $A_t^{[\Lambda,r,A_-]} = \bigcap_{\tau>0} \overline{\bigcup_{s<-\tau} \Phi(t, s, \mathcal{N}_\eta(A_-))}$ is bounded. Therefore, $A_t^{[\Lambda,r,A_-]}$ is compact for all $t \in \mathbb{R}$.

To prove $\mathcal{A}^{[\Lambda,r,A_-]}$ is invariant note that

$$\begin{aligned}
\Phi(t, s, A_s^{[\Lambda,r,A_-]}) &= \Phi\left(t, s, \bigcap_{\tau>0} \overline{\bigcup_{k<-\tau} \Phi(s, k, \mathcal{N}_\eta(A_-))}\right) \\
&= \bigcap_{\tau>0} \overline{\bigcup_{k<-\tau} \Phi\left(t, s, \Phi(s, k, \mathcal{N}_\eta(A_-))\right)} \\
&= \bigcap_{\tau>0} \overline{\bigcup_{k<-\tau} \Phi\left(t, k, \mathcal{N}_\eta(A_-)\right)} \\
&= A_t^{[\Lambda,r,A_-]}
\end{aligned}$$

for all $t > s$ (we use the property that $\Phi(t, s, \cdot)$ is a diffeomorphism for all t, s).

To show that $\mathcal{A}^{[\Lambda,r,A_-]}$ attracts an open set U in pullback sense, let $U = \mathcal{N}_\eta(A_-)$, $t \in \mathbb{R}$ with η as before, and define

$$B_{\tau,t} := \overline{\bigcup_{k<-\tau} \Phi(t, k, U)}.$$

Note that $A_t^{[\Lambda,r,A_-]} = \bigcap_{\tau>0} B_{\tau,t}$ and $B_{s,t} \subset B_{\tau,t}$ for any $\tau < s$. Moreover, $d(B_{\tau,t}, A_t^{[\Lambda,r,A_-]}) \to 0$ as $\tau \to \infty$. Using Lemma 4.2.3 we have that

$$\Phi(t, s, U) \subset B_{\tau,t}$$

for all sufficiently negative s (depending on t and τ). Hence for such s

$$d(\Phi(t, s, U), B_{\tau,t}) = 0$$

Hence

$$\lim_{s\to-\infty} d(\Phi(t,s,U),A_t)=0$$

and thus $\mathcal{A}^{[\Lambda,r,A_-]}$ is a pullback attractor. □

By Lemma 4.2.1, $A_{-\infty}^{[\Lambda,r,A_-]}$ is invariant for the past limit system, if A_- is minimal invariant set (for example, if it is an equilibrium or periodic orbit) then $A_{-\infty}^{[\Lambda,r,A_-]} = A_-$. We believe that $A_{-\infty}^{[\Lambda,r,A_-]} = A_-$ in more general cases but are not clear whether additional hypotheses are needed to prove this. We also note that the proof of Theorem 4.2.2 can be obtained by adapting [58, Theorem 2.35 and Corollary 2.36] to this setting.

Theorem 4.2.2 highlights that the backward limit of a pullback attractor for the parameter shift system (1.3) is related to an attractor of the past limit system. Whether the forward limit of the pullback attractors is related to an attractor of the future limit system is a more subtle question that relates directly to rate-dependent transitions.

4.3 Pullback attractors and rate-dependent phenomena

Based on Theorem 4.2.2, we consider the the upper forward limit of the pullback attractor (4.2) and define the following:

Definition 4.3.1. Suppose that $(A(\lambda),\lambda)\subset\mathcal{X}_{\text{stab}}$ is a branch of attractors that are exponentially stable for $\lambda\in[\lambda_-,\lambda_+]$. Define $A_\pm := A(\lambda_\pm)$ and consider the pullback attractor $\mathcal{A}^{[r,\Lambda,A_-]}$ with past limit $A_- = A(\lambda_-)$.

(i) We say there is (end-point) *tracking* for system (1.3) from A_- for some Λ and $r>0$ if $A_{+\infty}^{[\Lambda,r,A_-]}\subseteq A_+$.

   (a) We say there is *weak tracking* if $A_{+\infty}^{[\Lambda,r,A_-]}\subsetneq A_+$.

(b) We say there is *strong tracking* if $A_{+\infty}^{[\Lambda,r,A_-]} = A_+$.

(ii) We say there is *R-tipping* for system (1.3) from A_- for some Λ and $r > 0$ if $A_{+\infty}^{[\Lambda,r,A_-]} \not\subset A_+$.

(a) We say there is *partial tipping* if

$$(A_+)^C \cap A_{+\infty}^{[\Lambda,r,A_-]} \neq \emptyset, \quad \text{and} \quad A_+ \cap A_{+\infty}^{[\Lambda,r,A_-]} \neq \emptyset.$$

(b) We say there is *total tipping* if

$$A_+ \cap A_{+\infty}^{[\Lambda,r,A_-]} = \emptyset.$$

(iii) For given A_- and Λ there will be partition of the positive half axis into disjoint subsets: $\mathbb{R}_{\text{track}}$ where there is tracking, $\mathbb{R}_{\text{P}}$ where there is partial tipping and $\mathbb{R}_{\text{T}}$ where there is total tipping. i.e. $\mathbb{R}^+ = \mathbb{R}_{\text{track}} \cup \mathbb{R}_{\text{P}} \cup \mathbb{R}_{\text{T}}$ and $\mathbb{R}_{\text{track}} \cap \mathbb{R}_{\text{P}} = \mathbb{R}_{\text{track}} \cap \mathbb{R}_{\text{T}} = \mathbb{R}_{\text{P}} \cap \mathbb{R}_{\text{T}} = \emptyset$.

We define the *critical rates* or *thresholds for rate-induced transitions* as the boundaries of these subsets.

(iv) Assume that there is an $r_0 \in \mathbb{R}_P$ and some $r_{\min}$ and $r_{\max}$, such that $[r_{\min}, r_0) \cup (r_0, r_{\max}] \subset \mathbb{R}_{\text{track}}$. In this case we say the system has *invisible tipping* at r_0.

By analogy with Lemma 3.2.2 we expect for sufficiently small $r > 0$ that the pullback attractor will track (i.e. remain close to) the branch $A(\lambda)$. This is expressed more precisely in the following result.

Theorem 4.3.1. Suppose that $(A(\lambda), \lambda) \subset \mathcal{X}_{\text{stab}}$ is a branch of attractors that is uniformly stable for $\lambda \in [\lambda_-, \lambda_+]$ and suppose Λ is a parameter shift. Define $A_\pm = A(\lambda_\pm)$ and the pullback attractor $\mathcal{A}^{[\Lambda,r,A_-]}$ with fibres $A_t^{[\Lambda,r,A_-]}$ as in (4.2).

Then for all $\epsilon > 0$ there exists a $\delta > 0$ such that:

$$d\left(A_t^{[\Lambda,r,A_-]}, A(\Lambda(rt)\right) < \epsilon$$

for all $0 < r < \delta$ and $t \in \mathbb{R}$. Moreover, there is a $\delta > 0$ such that there is tracking for all $0 < r < \delta$.

Proof. Since $A(\lambda)$ is uniformly stable for all $\lambda \in [\lambda_-, \lambda_+]$ then there exist $\mu > 0$, $\eta > 0$ and $C \geq 1$ (which we fix from here on in the proof) such that

$$d\left(\phi_\lambda(t,x), A(\lambda)\right) < Ce^{-\mu t} d\left(x, A(\lambda)\right) \tag{4.3}$$

for all $x \in \mathcal{N}_\eta\left(A(\lambda)\right)$ and $t > 0$.

Pick any $0 < \epsilon < \eta$, consider any $t \in \mathbb{R}$ and $\lambda = \Lambda(rt)$. By (4.3) $d\left(\phi_\lambda\left(s,x\right), A(\lambda)\right) < \epsilon e^{-\mu s}/3$, for all $x \in \mathcal{N}_{\epsilon/C}\left(A(\Lambda(rt))\right)$ and $s > 0$. In particular, we can pick $s > 0$ independent of t such that $e^{-\mu s} = 1/C$ and so

$$\phi_\lambda\left(s, \mathcal{N}_{\epsilon/C}\left(A(\lambda)\right)\right) \subset \mathcal{N}_{\epsilon/(3C)}\left(A(\lambda)\right).$$

By the continuity of Φ, for all $s > 0$ and $t \in \mathbb{R}$ there exits $\delta_1 > 0$ such that for all $0 < r < \delta_1$ and $x \in \mathcal{N}_\epsilon(A(\lambda))$

$$\|\phi_\lambda(s,x) - \Phi(t+s,t,x)\| < \epsilon/(3C).$$

Again by the continuity of $A(\lambda)$ there exist $\delta_2 > 0$ such that for all $t \in \mathbb{R}$ and $0 < r < \delta_2$

$$d_H\left(A(\Lambda(r(t+s))), A(\lambda)\right) < \epsilon/(3C).$$

Now set $\delta = \min\{\delta_1, \delta_2\}$, then for all $x \in \mathcal{N}_{\epsilon/C}(A(\lambda))$, $t \in \mathbb{R}$ and $0 < r < \delta$,

$$\begin{aligned} d\left(\Phi\left(t+s,t,x\right), A\left(\Lambda\left(r(t+s)\right)\right)\right) &< d\left(\Phi(t+s,t,x), \phi_\lambda(s,x)\right) + d\left(\phi_\lambda(s,x), A(\lambda)\right) \\ &\quad + d\left(A(\lambda), A(\Lambda(r(t+s))\right) \\ &\leq \|\phi_\lambda(s,x) - \Phi(t+s,t,x)\| + d\left(\phi_\lambda(s,x), A(\lambda)\right) \\ &\quad + d_H\left(A\left(\Lambda(r(t+s))\right), A(\lambda)\right) \\ &< \epsilon/(3C) + \epsilon/(3C) + \epsilon/(3C) = \epsilon/C \end{aligned}$$

which follows from the triangle inequality for Hausdorff semi-distance, $d(u,v) = \|u - v\|$ for all $u, v \in \mathbb{R}^n$ and $d\left(A,B\right) \leq d_H\left(A,B\right)$ for all A, B compact subsets of $\mathbb{R}^n$. This means that for all $0 < r < \delta$ and $t \in \mathbb{R}$ there is an $s > 0$ such that

$$\Phi(t+s,t,\mathcal{N}_{\epsilon/C}(A(\Lambda(rt))) \subset \mathcal{N}_{\epsilon/C}(A(\Lambda(r(t+s))).$$

By Theorem 4.2.2, $A_{-\infty}^{[\Lambda,r,A_-]} \subset A_-$ which means for all $\epsilon > 0$ there is a $\tau > 0$ such that $d(A_t^{[\Lambda,r,A_-]}, A(\Lambda(rt))) < \epsilon/C$ for all $t < -\tau$. Therefore, for all $0 < \epsilon < \eta$ there exists a $\delta > 0$ such that for all $0 < r < \delta$ and $t \in \mathbb{R}$ we have

$$d\left(A_t^{[\Lambda,r,A_-]}, A(\Lambda(rt))\right) < \epsilon/3C.$$

To prove the second part of the theorem, we define

$$C_\tau = \overline{\bigcup_{s>\tau} A_s^{[\Lambda,r,A_-]}}.$$

Note that $C_u \subset C_\tau$ for any $u > \tau$ and $A_{+\infty}^{[\Lambda,r,A_-]} = \bigcap_{\tau>0} C_\tau$. Moreover we have $d_H(C_\tau, A_{+\infty}^{[\Lambda,r,A_-]}) \to 0$ as $\tau \to \infty$.

From before, for any $\epsilon > 0$ and $t \in \mathbb{R}$ there is $\delta > 0$ such that

$$d(A_t^{[\Lambda,r,A_-]}, A(\Lambda(rt))) < \epsilon/2C$$

for all $0 < r < \delta$.

Now from the fact that $d_H(A(\Lambda(rt)), A_+) \to 0$ as $t \to \infty$ and the definition of C_τ, we have $d(C_\tau, A_+) \to 0$ as $\tau \to \infty$. Hence, by the triangle inequality of Hausdorff semi-distance

$$d(A_{+\infty}^{[\Lambda,r,A_-]}, A_+) = 0.$$

This finishes the proof. □

Although Theorem 4.3.1 means that a pullback attractor will track a branch of "sufficiently stable" attractors for the associated autonomous system for small enough rates, there is no guarantee this holds for larger rates. R-tipping occurs precisely when tracking fails to occur.

Chapter 5

A model example with partial and total tipping

This chapter illustrates two of the phenomena that are stated in Definition 4.3.1 with one model example. Our example (5.3) has a branch or periodic attractors and exhibits partial and total tipping in addition to strong tracking.

Because of the minimality of the periodic attractor, system (5.3) can not exhibit weak tracking. This particular phenomenon may occur in systems where the attractors of the future limit systems are not minimal, see Chapter 6.

In Section 5.2 we argue that one can relate the pullback attractor to an invariant manifold, therefore the critical rate of partial or total tipping can be viewed as a tangency of this manifold with other manifolds. In other words, the critical rates of total, partial tipping are associated with codimension-one heteroclinic connections between two saddle objects for an augmented system.

In Section 5.3, we use Lin's approach to investigate these connections. Similar to [3], we have been able to define numerical bifurcation function ξ, where the heteroclinic connections are given by the zeros of ξ. By continuing these connections in two parameter plane, we identify the thresholds of partial and total tipping as well as regions of qualitatively different behaviour.

The main results of this chapter have been published in *Chaos: An Interdisciplinary Journal of Nonlinear Science* [1, Sections IV].

5.1 Bautin normal form with parameter shift

Consider the following (nonautonomous) system:

$$\dot{z} = F(z - \Lambda(rt)) \tag{5.1}$$

where $z = x+iy \in \mathbb{C}$, the parameter shift $\Lambda(\tau) = \lambda_{\max}\left(\tanh(\tau\lambda_{\max}/2) + 1\right)/2$ limits to 0 in the past and $\lambda_{\max}$ in the future, see Figure 1.4, and $F(z)$ is defined by

$$F(z) = (a + i\omega)z - b|z|^2 z + |z|^4 z \tag{5.2}$$

for a, b, ω, r and $\lambda_{\max} \in \mathbb{R}$, $r, \lambda_{\max} > 0$: we set $b = 1$ in what follows. Note that $\dot{z} = F(z)$ can be thought of a normal form for a Bautin bifurcation, where a Hopf bifurcation changes criticality at $b = 0$. One can view (5.1) autonomously as:

$$\begin{aligned} \dot{z} &= F(z - \Lambda) \\ \dot{\Lambda} &= r\Lambda(\lambda_{\max} - \Lambda). \end{aligned} \tag{5.3}$$

For $r = 0$ and any fixed Λ there are bifurcation points at $a = 0$ and $a = 0.25$, that are Hopf and fold of periodic orbits respectively. For $0 < a < 0.25$ the system has an unstable equilibrium point $Z(\lambda) := \lambda + 0i$, as well as both stable and unstable periodic orbit. We denote the radius of the unstable periodic orbit by $R_u := \sqrt{(1 + \sqrt{1 - 4a})/2}$ and the radius of the stable periodic orbit by $R_s := \sqrt{(1 - \sqrt{1 - 4a})/2}$. Note that the stable periodic orbit is $\Gamma^s(\lambda) := \{z \in \mathbb{C} : \|z - \lambda\|^2 = R_s^2\}$ and the unstable periodic orbit is $\Gamma^u(\lambda) := \{z \in \mathbb{C} : \|z - \lambda\|^2 = R_u^2\}$.

For a solution of (5.3) and $r > 0$ there are two stationary values of Λ: $\lambda_- = 0$ and $\lambda_+ = \lambda_{\max}$. Hence in general, there are six invariant sets associated with those two

Table 5.1: The equilibria and periodic orbits of system (5.3). $n_{c,u,s}$ denote to the dimensions number of the stable, unstable and the center manifolds.

The Invariant set	n_c	n_u	n_s	**Set type**
$Z_- = \{(0,0)\}$	0	3	0	unstable equilibrium
$\Gamma_-^u = \{z \in \mathbb{C} : \|z\| = R_u\}$	1	2	0	unstable periodic orbit
$\Gamma_-^s = \{z \in \mathbb{C} : \|z\| = R_s\}$	1	1	1	saddle periodic orbit
$Z_+ = \{(0, \lambda_{\max})\}$	0	2	1	saddle equilibrium
$\Gamma_+^u = \{z \in \mathbb{C} : \|z - \lambda_{\max}\| = R_u\}$	1	1	1	saddle periodic orbit
$\Gamma_+^s = \{z \in \mathbb{C} : \|z - \lambda_{\max}\| = R_s\}$	1	0	2	stable periodic

limiting values, and we denote them by Z_-, Γ_-^s and Γ_-^u associated with $\Lambda = \lambda_- = 0$ and Z_+, Γ_+^s and Γ_+^u associated with $\Lambda = \lambda_+ = \lambda_{\max}$. Table 5.1 summarises the stability of those six invariant sets.

Theorem 4.3.1 implies that the upper forward limit of the pullback attractor $\mathcal{A}^{[\Lambda, r, \Gamma_-^u]}$ is the attracting periodic orbit Γ_+^s of the future limit systems, for all small enough r. However, there can be up to three critical rates of r for all fixed values of the parameters $a, \omega, \lambda_{\max}$ that can give partial, total and even invisible tipping.

5.2 Pullback attractors, tipping, and invariant manifolds

Writing $W^u(X)$ to denote the unstable and $W^s(X)$ the stable manifold the hyperbolic invariant set X, note that $W^s(\Gamma_+^u)$ forms the basin boundary of Γ_+^s, and the branch of stable periodic orbits is uniformly stable.

The various cases of tracking and tipping can be understood in terms of the unstable manifolds of these invariant sets[7]. More precisely, the pullback attractor of (5.1) consists of sections of $W^u(\Gamma_-^s)$ for (5.3). We can classify the tracking/tipping

as follows:

- If $\Gamma^s_+ \subset W^u(\Gamma^s_-)$ then there is end point tracking of the branch of periodic solutions $\Gamma^s(\Lambda(rt))$.
- If $[\Gamma^s_+]^c \cap W^u(\Gamma^s_-) \neq \emptyset$ then there is tipping: if in addition $\Gamma^s_+ \cap W^u(\Gamma^s_-) = \emptyset$ then there is total tipping for this r, otherwise it is partial tipping.
- Hence, if r is a threshold between tracking and partial tipping or between partial and total tipping then

$$W^u(\Gamma^s_-) \cap W^s(\Gamma^u_+) \neq \emptyset$$

with a unique trajectory that has non-transverse intersection: more precisely this means that at a typical point $p \in W^u(\Gamma^s_-) \cap W^s(\Gamma^u_+)$ we have

$$\dim \left(T_p W^u(\Gamma^s_-) \cap T_p W^s(\Gamma^u_+) \right) = 2. \tag{5.4}$$

- If r such that

$$W^u(\Gamma^s_-) \cap W^s(Z_+) \neq \emptyset$$

then this is generically an isolated point in r, and hence a invisible tipping.

Figure 5.2 illustrates some examples of numerical approximations showing trajectories and the relation between the stable manifold of the unstable equilibrium and unstable periodic orbit and the pullback attractors.

5.3 R-tipping as a heteroclinic bifurcation

As outlined in Section 5.2, it is possible to find thresholds of rate-induced tipping by considering certain periodic orbit to periodic orbit orbit (PtoP) and periodic orbit to equilibrium (PtoE) heteroclinic connections, analogous to [57, Proposition 4.1]. An

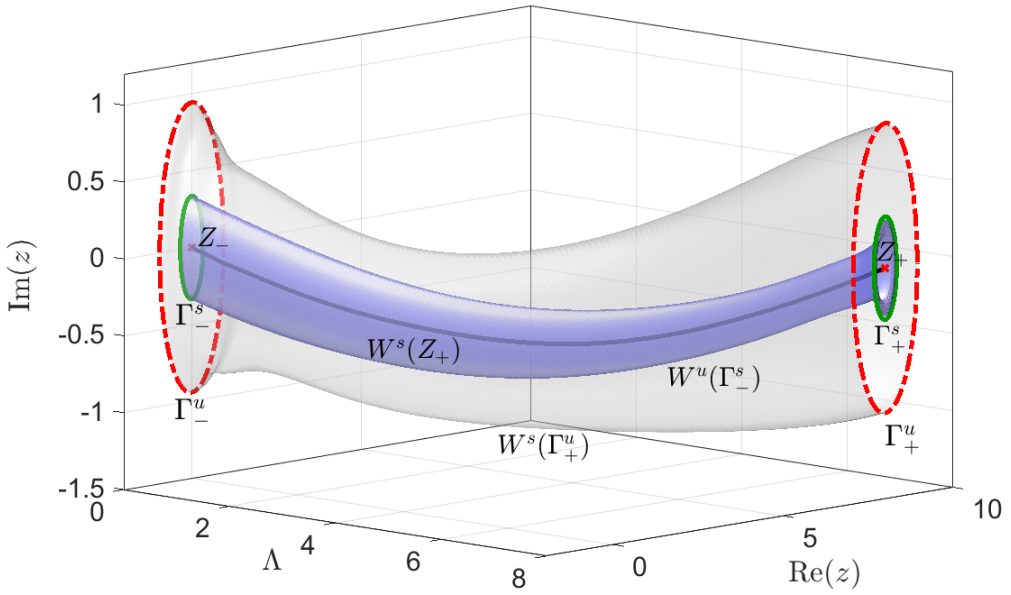

Figure 5.1: Numerical approximations of the pullback attractor $\mathcal{A}^{[\Lambda,r,\Gamma^s_-]}$ (for system (5.3)) for $a = 0.1$, $r = 0.1$, $b = 1$, $\lambda_{\max} = 8$ and $\omega = 3$. The graph of the pullback attractor (inner dark tube) over Λ is $W^u(\Gamma^s_-)$. In this case r is chosen small enough that there is tracking of the periodic attractor according to Theorem 4.3.1. The outer grey tube shows $W^s(\Gamma^u_+)$ whilst the inner black line is $W^s(X_+)$. The red circles indicate $\Gamma^u_\pm$, the green circles indicate $\Gamma^s_\pm$ and the red points indicate $Z_\pm$.

efficient way of doing this is Lin's method [25, 52] that involves solving three point boundary value problems with suitable boundary conditions that give the desired connection: see for example [33, 34, 29] for details.

On the other hand, the pullback attractor $\mathcal{A}^{[\Lambda,r,\Gamma^s_-]}$ can be approximated using a direct shooting method (see Figures 5.1 and 5.2). By determining the fate of the upper forward limit of $\mathcal{A}^{[\Lambda,r,\Gamma^s_-]}$, one can characterise different regions of tracking/tipping behaviour in (a, r)-parameter plane. Figure 5.4 shows that the results form both methods match quite well.

5.3.1 PtoP and PtoE connections by using Lin's method

Zhang *et al* [29] give a systematic method to find a PtoP connection where the intersection between the tangent space of the unstable and the stable manifold is

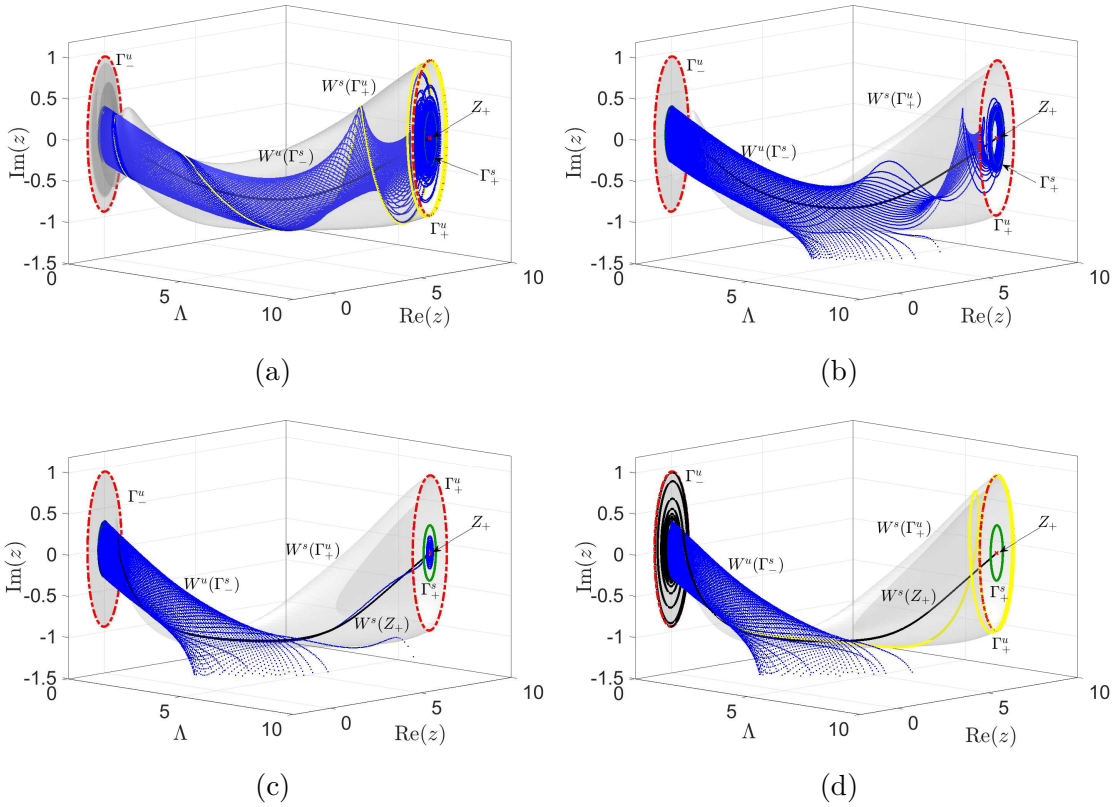

Figure 5.2: Numerical approximations of the pullback attractor as in Figure 5.1 but for different examples of tipping. (a) $r = 0.13321$ at the threshold of partial tipping: there is a single connection (yellow) in $W^u(\Gamma^s_-) \cap W^s(\Gamma^u_+)$ with non-transverse intersection. (b) $r = 0.15$ in the region of partial tipping: some of the trajectories in blue on the pullback attractor track while others escape. (c) $r = 0.198422$, showing existence of a PtoE connection (black). (d) $r = 0.201226$ showing total tipping.

one dimensional. However, for our critical rates even though the PtoP connection is one-dimensional, the intersection of the tangent spaces is of dimension two and solving [29, equations (6) - (11)] give criteria for codimension-zero connections. To find the critical rates of transition to partial and to total tipping we solve the adjoint variational equation (AVE) along the connection to allow us to test (5.4). Moreover, we replace [29, conditions (8) and (9)] by projection conditions (see for example (5.10)) in order to reduce the number of parameters in our BVP.

We fix $b = 1$, $\omega = 3$ and $\lambda_{\max} = 8$, and denote the system (5.3) by:

$$\dot{w} = G(w; \mu) \tag{5.5}$$

where $w(t) = (x(t), y(t), \Lambda(t)) \in \mathbb{R}^3$, $z(t) = x(t) + iy(t)$, $\mu = (a, r) \in \mathbb{R}^2$ and $G : \mathbb{R}^5 \to \mathbb{R}^3$ is the vector field of the system. The adjoint variational equation of a solution $w(t)$ of (5.5) at the parameter value μ_0 is given by [25]:

$$\dot{u} = -G_u(w, \mu_0)^{\mathrm{tr}} u \tag{5.6}$$

with solution $u(t)$, where $G_u(w, \mu_0)$ is the Jacobian matrix of the function $G(., \mu_0)$ over w and A^{tr} is the transpose of the matrix A. Let us assume that $T > 0$ is a (sufficiently large) integration time, $g_1(\vartheta) \in \Gamma^s_-$, $g_2(\varphi) \in \Gamma^u_+$, $\gamma^{\pm}_{s,c,u}$ give the stable/center/unstable eigendirections of Γ^s_-, Γ^u_- respectively for $0 < \vartheta$, $\varphi < 2\pi$, and $v_{1,2u}$ are the unstable eigenvectors of Z_+.

We consider some Lin problems for our system where there are connections between the saddle objects Γ^s_- and Γ^u_+ and Z_+. We are looking for connections between Γ^s_- in the past and Γ^u_+, Z_+ on the future. The unstable and stable manifold, $W^u(\Gamma^s_-)$ and $W^s(\Gamma^u_+)$, $W^s(Z_+)$ are of dimensions 2, 2 and 1 respectively. Assuming there exist a connection Q then for all point $q \in Q$ we have the following:

$$\dim \Big(T_q W^u(\Gamma^s_-) \bigcap T_q W^s(\Gamma^u_+) \Big) = 2,$$

$$\dim \Big(T_q W^u(\Gamma^s_-) \bigcap T_q W^s(Z_+) \Big) = 1.$$

We set the Lin section Σ, which is two dimensional linear space, half way between the asymptotic values of Λ:

$$\Sigma = \Big\{ w \in \mathbb{R}^3 : \Big\langle w - (0, 0, \lambda_{\max}/2), (0, 0, 1) \Big\rangle = 0 \Big\}.$$

The connection orbit Q intersects Σ transversely. i.e. $Q = Q^- \bigcup Q^+$ where:

$$Q^- = \{ w^-(t) : t \leq 0 \} \subset W^u(\Gamma^s_-) \quad \text{where} \quad w^-(1) \in \Sigma,$$

$$Q^+ = \{w^+(t) : t \geq 0\} \subset W^s(\Gamma^u_-) \quad \text{where} \quad w^+(0) \in \Sigma.$$

Now we define the "Lin gap" $\eta := w^-(1) - w^+(0) \in \Sigma$. Lin's method require that η lies in a fixed $d \leq \dim(\Sigma) - 1$ dimensional linear space L, which satisfies the following condition,[34]

$$\dim(W^- \oplus W^+ \oplus L) = \dim(\Sigma) \tag{5.7}$$

where $W^- = T_{w^-(0)}W^u(\Gamma^s_-) \bigcap T_{w^-(0)}\Sigma$ and $W^+ = T_{w^+(0)}W^s(\Gamma^u_+) \bigcap T_{w^+(0)}\Sigma$. The choice of L could be done by considering the adjoint variational equation along the solution Q [29], however the Lin space can be chosen arbitrarily as long as (5.7) is satisfied. The definitions of Q^- and Q^+ as well as condition (5.7) are formulated to investigate the PtoP connection between Γ^s_- and Γ^u_+. However, it still applicable to the PtoE connection between Γ^s_- and Z_+ with changing Γ^u_+ to Z_+ in each of them.

Note we also need approximations of the eigendirections for the periodic orbits: given a periodic solution $\Gamma = \{g(t) : 0 < t < T_\Gamma\}$ of the system (5.5) with period T_Γ, the eigendirections $\gamma_{s,c,u}$ and Floquet multiplies $\beta_{s,c,u}$ are obtained as solutions of

$$\begin{aligned} \dot{\gamma}_{s,c,u} &= T_\Gamma \, G_u(g(s);\mu)\gamma_{s,c,u}, \\ \gamma_{s,c,u}(1) &= \beta_{s,c,u} \, \gamma_{s,c,u}(0), \qquad\qquad 1 = \Big\langle \gamma_{s,c,u}(0), \gamma_{s,c,u}(0) \Big\rangle. \end{aligned} \tag{5.8}$$

for $0 < s < 1$.

We can write the BVPs of the relevant connections as the following:

We locate and continue a PtoE connection $W^u(\Gamma^s_-) \cap W^s(X_+) \neq \emptyset$ (corresponding to invisible tipping) by choosing a section $\Lambda = \lambda_{\max}/2$ and a Lin basis vector ℓ and solving

$$\dot{w}^-(s) = TG(w^-(s);\mu), \qquad \dot{w}^+(s) = TG(w^+(s);\mu), \tag{5.9}$$

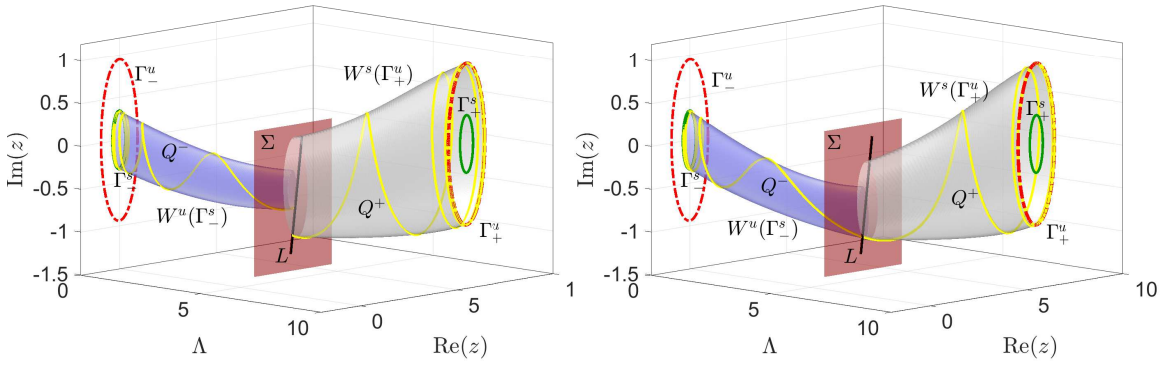

(a) (b)

Figure 5.3: Illustration of Lin's method for PtoP connection for (5.3). (a) shows that Lin's gap is grater than zero along L, for some values of the paramter $r \neq r_c$. Wilest, (b) shows that the PtoP connection for $r = r_c$ which is qiven by $Q = Q^- \cup Q^+$.

on $0 < s < 1$ with $T > 0$ sufficiently large and boundary conditions

$$\begin{aligned} 0 &= \left\langle w^-(0) - g_1(\vartheta), \gamma_s^-(\vartheta) \right\rangle, & 0 &= \left\langle w^-(0) - g_1(\vartheta), \gamma_c^-(\vartheta) \right\rangle, \\ 0 &= \left\langle w^+(1) - Z_+, v_{1u} \right\rangle, & 0 &= \left\langle w^+(1) - Z_+, v_{2u} \right\rangle, \\ 0 &= \left\langle w^-(1) - (0,0,\lambda_{\max}/2), (0,0,1) \right\rangle, & \xi\ell &= w^+(0) - w^-(1). \end{aligned} \tag{5.10}$$

We locate a codimension zero PtoP connection in $W^u(\Gamma^s_-) \cap W^s(\Gamma^u_+)$ by similarly choosing a section $\Lambda = \lambda_{\max}/2$ and solving

$$\dot{w}^-(s) = TG(w^-(s);\mu) \qquad \dot{w}^+(s) = TG(w^+(s);\mu), \tag{5.11}$$

on $0 < s < 1$ for some sufficiently large $T > 0$ with boundary conditions

$$\begin{aligned} 0 &= \left\langle w^-(0) - g_1(\vartheta), \gamma_s^-(\vartheta) \right\rangle, & 0 &= \left\langle w^-(0) - g_1(\vartheta), \gamma_c^-(\vartheta) \right\rangle, \\ 0 &= \left\langle w^-(1) - g_2(\varphi), \gamma_u^+(\varphi) \right\rangle, & 0 &= \left\langle w^-(1) - g_2(\varphi), \gamma_c^+(\varphi) \right\rangle, \\ 0 &= \left\langle w^-(1) - (0,0,\lambda_{\max}/2), (0,0,1) \right\rangle, & \xi\ell &= w^+(0) - w^-(1). \end{aligned} \tag{5.12}$$

This can be extended to find the codimension one PtoP connection (corresponding to a boundary between partial tipping and either tracking or total tipping) by solving

(5.11,5.12) and in addition the adjoint variational equation

$$\dot{u}^-(s) = -TG_u(w^-(s),\mu)^{\mathrm{tr}}u^-(s) \qquad \dot{u}^+(s) = -TG_u(w^+(s),\mu)^{\mathrm{tr}}u^+(s) \tag{5.13}$$

with boundary conditions

$$\begin{aligned} 0 &= \left\langle u^-(0), \gamma_u^-(\vartheta)\right\rangle, \quad 0 = \left\langle u^-(0), \gamma_c^-(\vartheta)\right\rangle, \\ 0 &= \left\langle u^+(1), \gamma_s^+(\varphi)\right\rangle, \quad 0 = \left\langle u^+(1), \gamma_c^+(\varphi)\right\rangle, \\ 0 &= u^-(1) - u^+(0), \quad 1 = \left\langle u^-(1), (1,0,0)\right\rangle. \end{aligned} \tag{5.14}$$

We implement this method as follows:

- Solving (5.8) numerically by using the MATLAB solver bvp5c gives the eigendirections for Γ_-^s and Γ_+^u which can be used to formulate the projection conditions in (5.10, 5.12, 5.14).
- We formulate the solution of (5.9, 5.11) as MATLAB function that return $\xi(r,a)$ using the MATLAB solver bvp5c. We use $(0,1,0)$ as a basis for the Lin space L.
- We consider $\xi : \mathbb{R}^2 \to \mathbb{R}$ as smooth real valued function that by finding its zero one can find the desired connections. We do this by using Newton-Raphson iteration with tolerance 10^{-5} and defining the derivative of ξ by finite difference with step size 10^{-4}.
- Continuing the zero set of $\xi(r,a)$ in the (a,r)-plane by pseudo-arclength continuation gives the curves in Figures 5.4b and 5.4c.

Solving the system (5.11,5.12,5.13,5.14) allows one to determine and continue the codimension-one PtoP connections that give the thresholds of partial and total tipping. As initial solution we solve the codimension-zero problem (5.11,5.12) and continuing it along r to arrive at a fold where the codimension-one connection exists. Figure 5.4 illustrates (a,r)-parameter plan for (5.3) in the case $b = 1$, $\omega = 3$

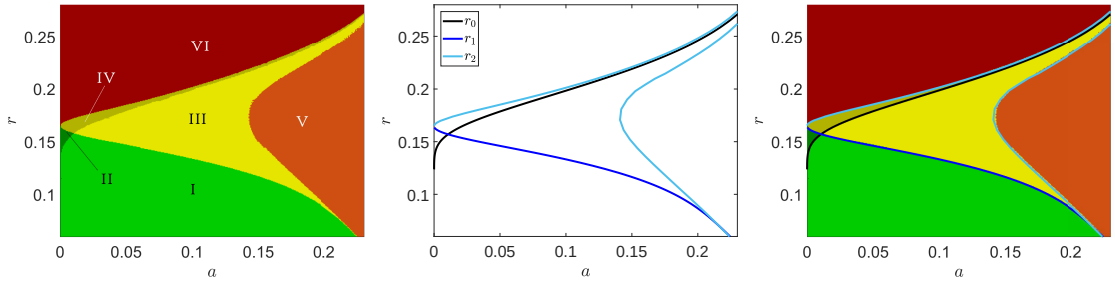

(a) (b) (c)

Figure 5.4: The two parameter plane of system (5.3) showing regions of different tracking/tipping behaviour (a) is calculated by directly approximating a collection of initial conditions on the pullback attractor and determining their fate under the dynamics of the system and shows six regions where the system has qualitatively different behaviour (see Figure 5.5). The curves in (b) are calculated using Lin's method and show the locations of these transitions: $r_{1,2}$ are the thresholds of partial and total tipping respectively and r_0 gives PtoE connection causing a invisible tipping for $0 < a < 0.0157$. In (c) they are superimposed.

and $\lambda_{\max} = 8$ calculated by Lin's method and compares it with a direct shooting algorithm described in Subsection 5.3.2. Figure 5.5 shows the behaviour of (5.3) in each different region of the parameter plan by looking at a section of the manifolds $W^u(\Gamma^s_-)$, $W^s(\Gamma^u_+)$ and $W^s(Z_+)$.

5.3.2 Tracking regions by using shooting method

The tracking/tipping regions of (5.3) shown in Figure 5.4a and 5.4c are found using a direct shooting method. The shooting method is a numerical method of solving boundary value problems by reducing them to initial value problems [46]. For the tracking/tipping regions of system (5.3) we can describe our shooting method as follows:

- We start with M evenly spaced initial conditions near the periodic orbit Γ^s_- and integrate (5.3) forward in time using ode45 MATLAB solver. We vary M depending on the value of r. As r increases it become difficult to determine partial tipping. Therefore, we increase M gradually from 200 when $r \approx 0.06$ to 20000 when $r \geq 0.24$ to compute the partial tipping region in Figure 5.4a

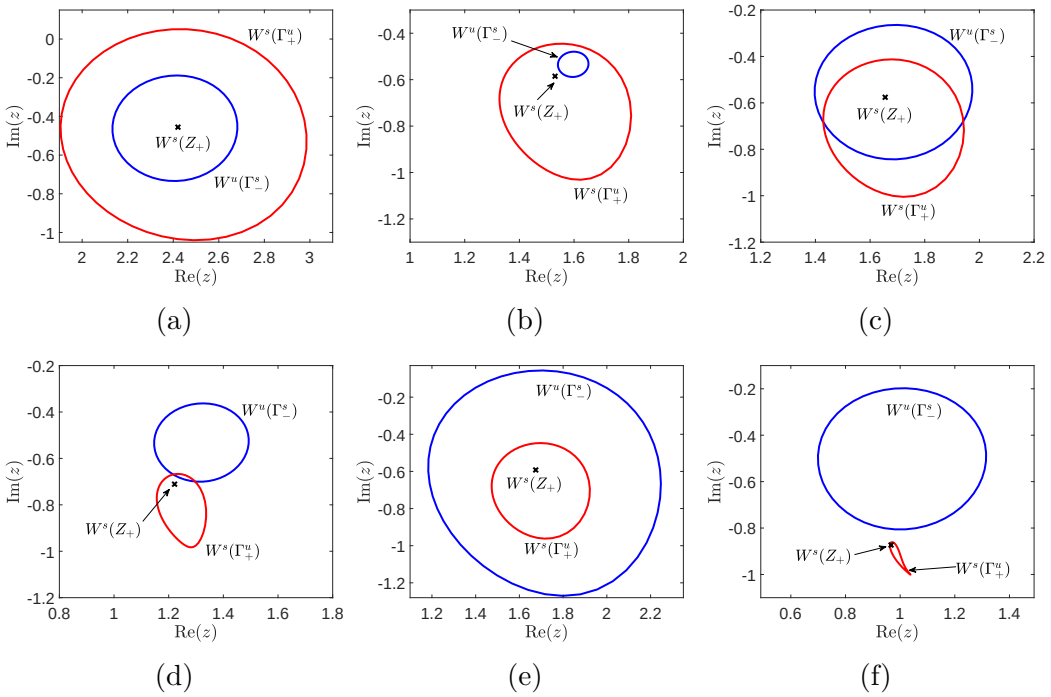

Figure 5.5: A section (fixed $\Lambda \approx 1.257$) of the manifolds $W^u(\Gamma^s_-)$ (in blue). $W^s(\Gamma^u_+)$ (in red) and $W^s(Z_+)$ (in black) showing the topological behaviours of their stable intersections for regions I-VI shown in Figure 5.4a. The values of the parameters are (a) $a = 0.1$, $r = 0.1$ region I, (b) $a = 0.005$,$r = 0.157$ region II, (c) $a = 0.1$, $r = 0.15$ region III, (d) $a = 0.04$, $r = 0.18$ region IV, (e) $a = 0.2$, $r = 0.15$ region V and finally (f) $a = 0.1$, $r = 0.21$ region VI.

effectively.

- Considering a large $T > 0$, we require $s \leq \Lambda(t) \leq (\lambda_{\max} - s)$ for $t \in [-T, T]$ for some small real number s. In our computations we set $s = 0.01$ which effectively determines T: for the parameter shift $\Lambda(\tau) = \frac{\lambda_{\max}}{2}\left(\tanh\left(\frac{\tau\lambda_{\max}}{2}\right) + 1\right)$, the integration time T can be given as $T = \ln\left(\frac{\lambda_{\max}-s}{s}\right)/(r\lambda_{\max})$ (note however that this will be inadequate near the bifurcations $a = 0$ and 0.25, as noted in the text).

- We determine which of the M trajectories approach Γ^u_+ by measuring the distance between the end point of each trajectory and the equilibrium point Z_+.

- The stable manifold of Z_+, $W^s(Z_+)$, can be computed as initial value problem

of the time reversed system (5.3) with initial condition $(\lambda_{\max}, 0, \lambda_{\max} - s)$.

- The regions of tracking, partial tipping, and total tipping, and whether $W^s(Z_+)$ limits to Z_- or Γ^u_- in the past, are used to characterize six different regions where the behaviour of the system is qualitatively different. These regions are shown in Figure 5.4a and the behaviour of the system at each of them is illustrated in Figure 5.5.

Chapter 6

Weak tracking of pullback attractors

Recall that Definition 4.3.1(i) says the pullback attractor $\mathcal{A}^{[\Lambda,r,A_-]}$ shows weak (end-point) tracking if its upper forward limit $A_{+\infty}^{[\Lambda,r,A_-]}$ included as a proper subset of A_+, which is the attractor of the future limit system that is Λ-connected to A_-. In fact, this type of behaviour requires a sense of non-minimality for the attractor A_+ of the future limit system.

For autonomous dynamical systems, an invariant set M is called a *minimal invariant set* if it has no proper invariant subset [38]. Analogously, an attractor A is called a *minimal attractor* if it has no proper sub-attractors [50]. To exhibit weak tracking, the attractor of the future limit system does not need to be a non-minimal attractor, it is sufficient to be non-minimal invariant set, as we show in Section 6.2. Note that $A_{+\infty}^{[\Lambda,r,A_-]}$ does not need to be an attractor in general, but Lemma 4.2.1 shows that it has to be an invariant set for the future limit system.

Even minimal chaotic attractors provide a rich source of attractors that are non-minimal invariant. Most chaotic attractors, such as Rössler attractor, have embedded unstable periodic orbits [41]. Although chaotic attractors for parameter shift systems have so far not received much attention in the literature, there is a

number of studies who have considered systems with a time-dependent parameter that pass through chaotic regions. Kaszás *et al* [27] have studied the equation of the forced pendulum with time-dependent amplitude of forcing. Although, they have shown that there is an analogy between the behavior of the pullback attractor of the nonautonomous system and the bifurcation diagram of the "frozen-in system", the structure of the fibres of the pullback attractor may be very complex even for parameter values where is no stable chaos. In another paper, Kaszás *et al* [28] have explored the time-dependent topology for the same system, showing that it can be described by pullback saddles and their unstable foliations.

Weak tracking of non-minimal invariant set may associate with some isolated critical values of $r > 0$, at which the upper forward limit $A_{+\infty}^{[\Lambda,r,A_-]}$ of the pullback attractor $\mathcal{A}^{[\Lambda,r,A_-]}$ is a proper subset of A_+. In this sense, weak tracking of non-minimal invariant sets is similar to invisible tipping (Definition 4.3.1 iv), where the tipping occurs at some isolated values of the parameter r. However, the key difference between them is that weak tracking requires the upper forward limit of the pullback attractor $A_{+\infty}^{[\Lambda,r,A]}$ to be properly included in the attractor of the future limit system A_+.

Section 6.1 presents an example that has non-minimal attractors for the future and the past limit systems. The example exhibits weak tracking for a whole range of $r > 0$, and not only some isolated values. The system we treat is a modified version of (5.3), where we vary ω with respect to time, such that it is asymptotic to zero when time tends to $\pm\infty$. This variation allows the future and the past limit systems to have non-minimal attractors, which are manifolds of stable equilibria $M_\pm$. The quasi-static systems however, have periodic orbit attractors, as $\omega \neq 0$.

Section 6.2 illustrates weak tracking in Rössler system [66]. The Rössler attractor is a minimal chaotic attractor that contains many unstable periodic orbits [12], which means it is not minimally invariant. For (6.5), we fix $b = 0.2$, $c = 5.7$ and shift a from -0.2, where the system has a stable equilibria Z_-, to 0.2 where the system has

a chaotic attractor A_+. For almost any value of r the pullback attractor $\mathcal{A}^{[\Lambda,r,Z_-]}$ of (6.5) has an upper forward limit equals to the whole chaotic attractor of the future limit system. Nevertheless, by targeting a specific saddle periodic orbit Γ_+ within A_+, we provide numerical evidence for weak tracking at isolated values of r. Furthermore, our observations suggest that there is a dense set of critical values in r-parameter space that gives weak tracking, but we conjecture this set has zero Lebesgue measure.

6.1 An example with non-minimal attractivity

Consider the nonautonomous system given by (5.1), where F is defined by (5.2), but for time-dependent oscillation frequency $\omega(\tau)$ that is given by:

$$\omega(\tau) = c\Lambda(\tau)\Big(\lambda_{\max} - \Lambda(\tau)\Big),$$

where Λ is a parameter shift given by $\Lambda(\tau) = \lambda_{\max}\left(\tanh(\tau\lambda_{\max}/2) + 1\right)/2$ and $c, r, \lambda_{\max} \in \mathbb{R}$ with $r, \lambda_{\max} > 0$.

The augmented (four-dimensional system) can be given as:

$$\begin{aligned} \dot{z} &= F(z - \Lambda), \\ \dot{\Lambda} &= r\Lambda(\lambda_{\max} - \Lambda), \\ \dot{\omega} &= c\Lambda(\lambda_{\max} - \Lambda)(\lambda_{\max} - 2\Lambda), \end{aligned} \tag{6.1}$$

where $\dot{z} = F(z)$ is the normal form of Bautin bifurcation, which is defined by (5.2). Note that: because that Λ is asymptotic to 0 and $\lambda_{\max}$ as time tends to $\pm\infty$, ω is asymptotic to 0 as time tends to $\pm\infty$, see Figure 6.1.

Having zero oscillation frequency for the limit systems means that they have a manifold of attracting equilibria. The non-minimality of the manifolds of equilibria allow the system to exhibit weak tracking for some range of $r > 0$, see Figure

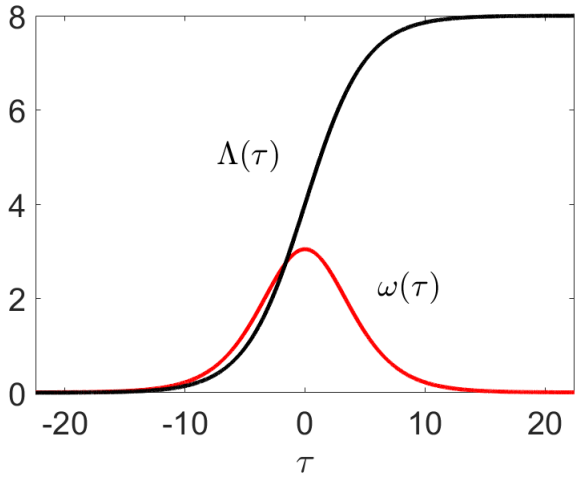

Figure 6.1: ω and Λ for system (6.1) vary with time.

6.3. We argue that there is a critical rate for weak tracking that is associated with heteroclinic bifurcation for the augmented system (6.1).

To analyse the the dynamics of the past limit system of (6.1) we set $\omega = \Lambda = 0$ and assume that $z = \rho e^{i\theta}$. By substituting in (6.1) we get:

$$\left.\begin{aligned} \dot{\rho} &= a\rho - \rho^3 + \rho^5 - r\Lambda(\lambda_{\max} - \Lambda)\cos(\theta), \\ \dot{\theta} &= \omega + r\Lambda(\lambda_{\max} - \Lambda)\sin(\theta)/\rho, \\ \dot{\Lambda} &= r\Lambda(\lambda_{\max} - \Lambda), \\ \dot{\omega} &= c\Lambda(\lambda_{\max} - \Lambda)(\lambda_{\max} - 2\Lambda), \end{aligned}\right\} \tag{6.2}$$

the past limit system is given where θ is static i.e:

$$\left.\begin{aligned} \dot{\rho} &= a\rho - \rho^3 + \rho^5, \\ \dot{\theta} &= 0. \end{aligned}\right\} \tag{6.3}$$

In addition to the equilibrium point $Z_- = (0, 0)$, there are two more invariant sets for the system that are both manifolds of equilibria,

$$M_-^s = \{(R_s, \theta) \in \mathbb{R} \times [0, 2\pi]\} = \{z \in \mathbb{C} : \|z\| = R_s\}$$

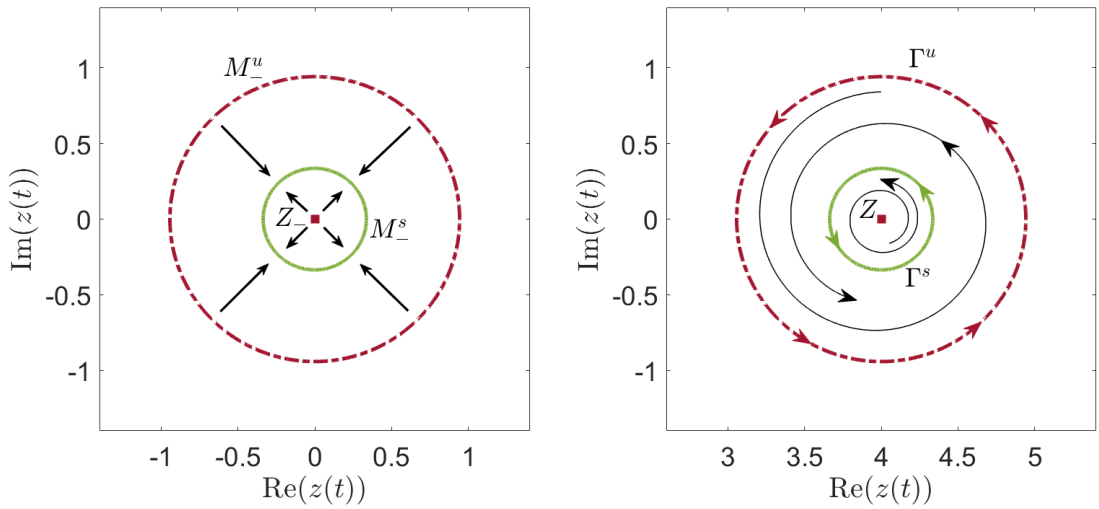

(a) (b)

Figure 6.2: The phase portrait of the past limit and associated autonomous systems of (6.1). (a) is the past limit phase portrait with parameter value $a = 0.1$, one can see that there is no rotation (i.e no θ-dynamics in (6.3)). (b) shows the phase portrait of the associated autonomous system for the same value of a and fixed $\lambda = 4$ and $\omega \approx 3.046$.

and

$$M_-^u = \{(\mathbb{R}_u, \theta) \in \mathbb{R} \times [0, 2\pi]\} = \{z \in \mathbb{C} : \|z\| = R_u\},$$

where R_s and R_u are the same as in Section 5.1. Similarly, one can find the invariant objects for the future limit system, which are again an equilibria $Z_+ = (\lambda_{\max}, 0)$ and two manifold of equilibria

$$M_+^s = \{z \in \mathbb{C} : \|z - \lambda_{\max}\| = R_s\},$$

and

$$M_+^u = \{z \in \mathbb{C} : \|z - \lambda_{\max}\| = R_u\},$$

who are stable and unstable respectively. Figure 6.2a shows the phase portrait of the past limit system, which is qualitatively the same as the phase portrait of the future limit system.

Whilst there is no θ-dynamics for the past and future limit systems, as $\omega = 0$,

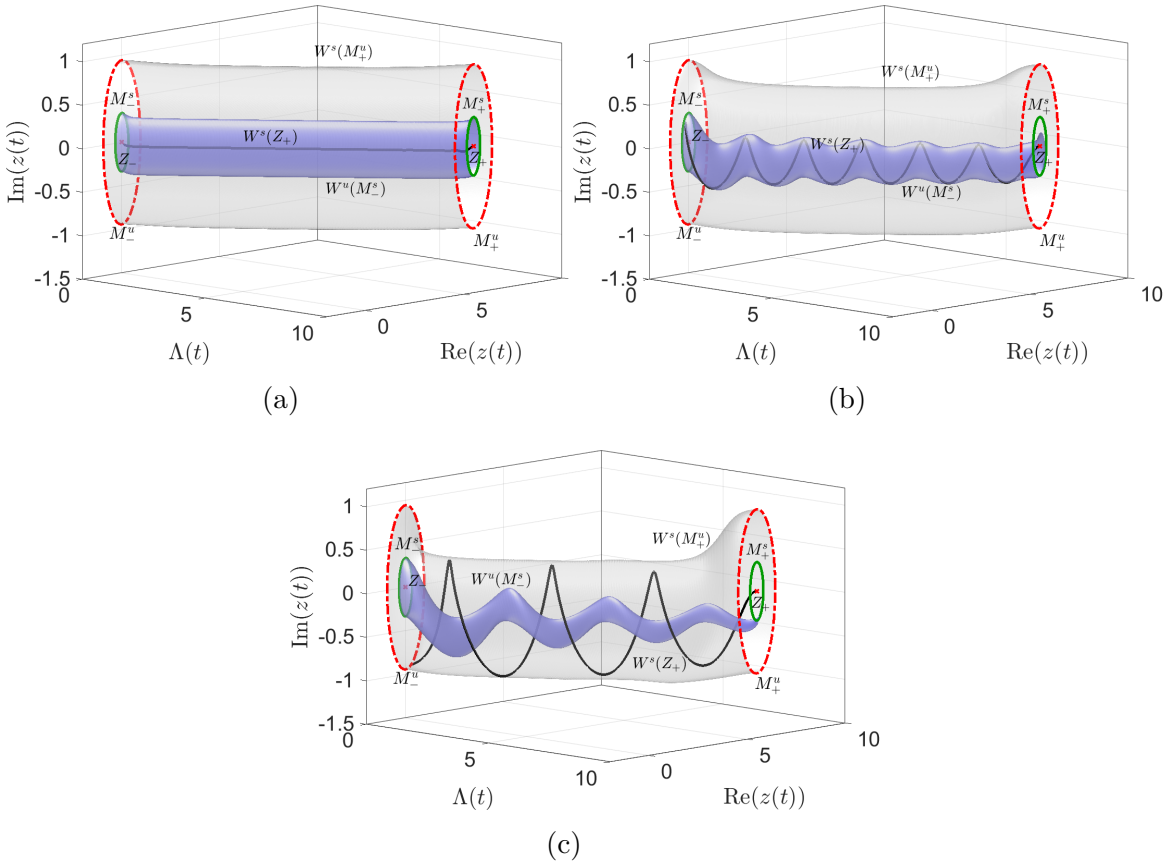

Figure 6.3: Numerical simulation of the pullback attractor $\mathcal{A}^{[\Lambda,r,M_-^s]}$ (inner dark blue tube) of (6.1) shows weak and strong tracking. The gray tube represents $W^s(M_u)$ the stable manifold of M_u^+. The black solid curve represent the stable manifold of Z_+ . The sub-figure (a) shows strong tracking $r = 0.01$; (b) shows the threshold of weak tracking $r = r_w \approx 0.0399$ as it can be seen that there is a heteroclinic connection between Z_+ and M_-^s; and (c) shows weak tracking $r = 0.07$. The other parameter values are fixed at $a = 0.1$, $\lambda_{\max} = 8$ and $c = 0.19$.

the associated autonomous systems have non-trivial dynamics of θ. Since for any real t we have $\omega(rt) \neq 0$, the associated autonomous systems have a stable and unstable periodic orbit defined similarly to these in Section 5.1. i.e:

$$\Gamma^s(\lambda) = \{z \in \mathbb{C} : \|z - \lambda\| = R_s\}$$

and

$$\Gamma^u(\lambda) = \{z \in \mathbb{C} : \|z - \lambda\| = R_u\},$$

where $\lambda = \Lambda(rt)$ for all $t \in \mathbb{R}$.

Similar to Section 5.2, we argue that the pullback attractor $\mathcal{A}^{[\Lambda,r,M^s_-]}$ consists of sections of the unstable manifold $W^u(M^s_-)$ of the attractor of the past limit system M^s_-, recall that M^s_- is a saddle with respect to the augmented system (6.1). Moreover, assume that there is ongoing weak tracking for some $r > 0$. Then there is $r_w > 0$ at which the system has codimension 1 heteroclinic connection between M^s_- and Z_+. We call r_w the *critical rate of weak tracking*. Figure 6.3 (b) illustrates this connecting orbit.

For any $r > r_w$ the pullback attractor $\mathcal{A}^{[\Lambda,r,M^s_-]}$ shrinks significantly and rotates slowly around the quasi-static equilibrium, see Figure 6.3c. Therefore, the sufficient condition for system (6.2) to exhibit weak tracking is to have the pullback attractor stop rotating eventually (i.e. $\theta \to L$ as $t \to \infty$ for some $L \in \mathbb{R}$). It is clear that $\dot{\theta} \to 0$ as $t \to \infty$, therefore, to show that θ is really asymptotic to a finite value L we need to show it is bounded.

$$\begin{aligned}
\dot{\theta} &= \omega + r\Lambda(\lambda_{\max} - \Lambda)\sin(\theta)/\rho, \\
&= c\Lambda(\lambda_{\max} - \Lambda) + r\Lambda(\lambda_{\max} - \Lambda)\sin(\theta)/\rho, \\
&= r\Lambda(\lambda_{\max} - \Lambda)\left(c/r + \sin(\theta)/\rho\right), \\
&= \dot{\Lambda}\left(c/r + \sin(\theta)/\rho\right).
\end{aligned}$$

Note that $|\sin(\theta)| \leq 1$, and for the pullback attractor $\mathcal{A}^{[\Lambda,r,M^s_-]}$ ρ is a constant and equals to R_s. Hence for all positive real t we have

$$\begin{aligned}
|\dot{\theta}| \leq \dot{\Lambda}\left(c/r + 1/R_s\right) &\implies \int_0^t |\dot{\theta}| ds \leq \int_0^t \dot{\Lambda}\left(c/r + 1/R_s\right) ds, \\
&\implies |\theta(t) - \theta(0)| \leq |\Lambda(t) - \Lambda(0)|\left(c/r + 1/R_s\right), \\
&\implies |\Lambda(t) - \Lambda(0)| \leq \lambda_{\max}\left(c/r + 1/R_s\right).
\end{aligned}$$

6.2 Weak tracking for a nonautonomous Rössler system

In 1976, Otto Rössler [66, 67] proposed one of the simplest systems of ODEs that can behave chaotically. Rössler's system, which has only one non-linear term, is given by:

$$\begin{aligned} \dot{x} &= -y - z, \\ \dot{y} &= x + ay, \\ \dot{z} &= b + z(x - c). \end{aligned} \tag{6.4}$$

There are many choices of a, b and c that gives chaotic attractor [2, 8, 40]. However, the most common parameter values are $a = b = 0.2$ and $c = 5.7$ that have been used by Rössler himself in [66], the chaotic attractor for these typical parameter values is shown in Figure 6.4.

We fix $b = 0.2$ and $c = 5.7$ throughout and analyse the bifurcations of (6.4) with respect to a. The system has two equilibria [12] that are given as:

$$p_{1,2} = (x_{1,2}, y_{1,2}, z_{1,2}) = \frac{c \pm \sqrt{c^2 - 4ab}}{2a} (a, -1, 1) .$$

We are interested in the bifurcation of the first equilibria, which is asymptotically stable for any negative a and bifurcates to stable periodic orbit at supercritical Hopf bifurcation point $a_{HB} \approx 0.005978$. Soon after Hopf bifurcation, the resulting stable periodic orbit exhibits period doubling at $a_{\text{PD}} = 0.1096$, and a period doubling cascade as a increases until the system exhibit chaotic behaviour at $a \approx 0.155$, see Figure 6.6.

6.2.1 The return map of Rössler system

The Poincaré return map is a powerful technique to analyse and understand the bifurcations of periodic orbits. The technique involves choosing a suitable Poincaré

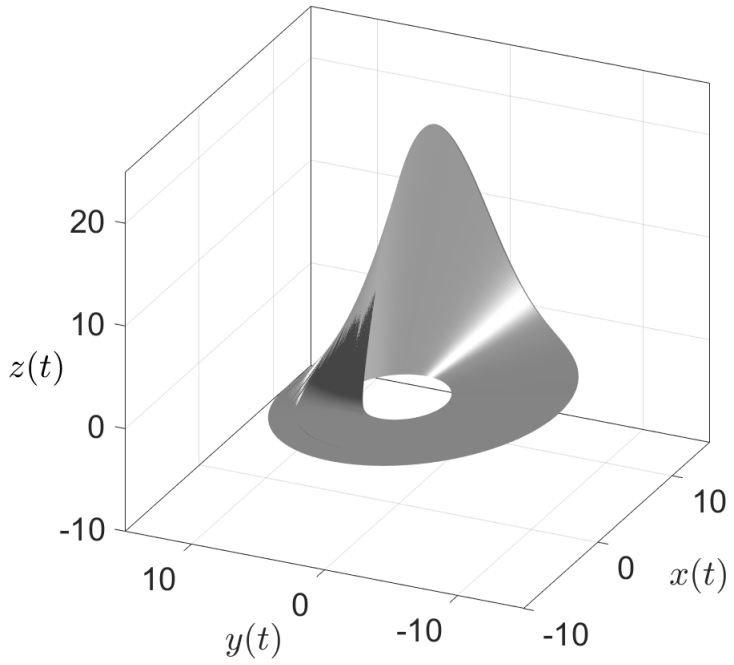

Figure 6.4: Rössler attractor for the typical parameter values $a = b = 0.2$ and $c = 5.7$.

section Σ [24] and reduces the flow to a map by considering the intersection points of the trajectories with Σ, see Figure 6.5b. In general, the dimension of Σ is one less than the dimension of the state space; i.e. Σ is of codimension-one [37]. Although, there are many ways of choosing Poincaré section for (6.4) [12, 40], we define the section as the following:

$$\Sigma := \left\{(x, y, z) \in \mathbb{R}^3 : x = -y, x \geq 0\right\},$$

which can be seen in Figure 6.5. The return map $M : \Sigma \to \Sigma$ is defined as the following. For a trajectory $(x(t), y(t), z(t))$ that intersect Σ at time t_n for $n = 1, 2, ...$ i.e $(x(t_n), -x(t_n), z(t_n)) \in \Sigma$ for $n = 1, 2, ...$, for short we denote $x(t_n)$ and $z(t_n)$ by x_n and z_n respectively. The return map M maps (x_{n-1}, z_{n-1}) into (x_n, z_n).

Strogatz [76] argues that the return map of Rössler's system behaves like a one-dimensional unimodal map and so Feigenbaum's universality theory can be

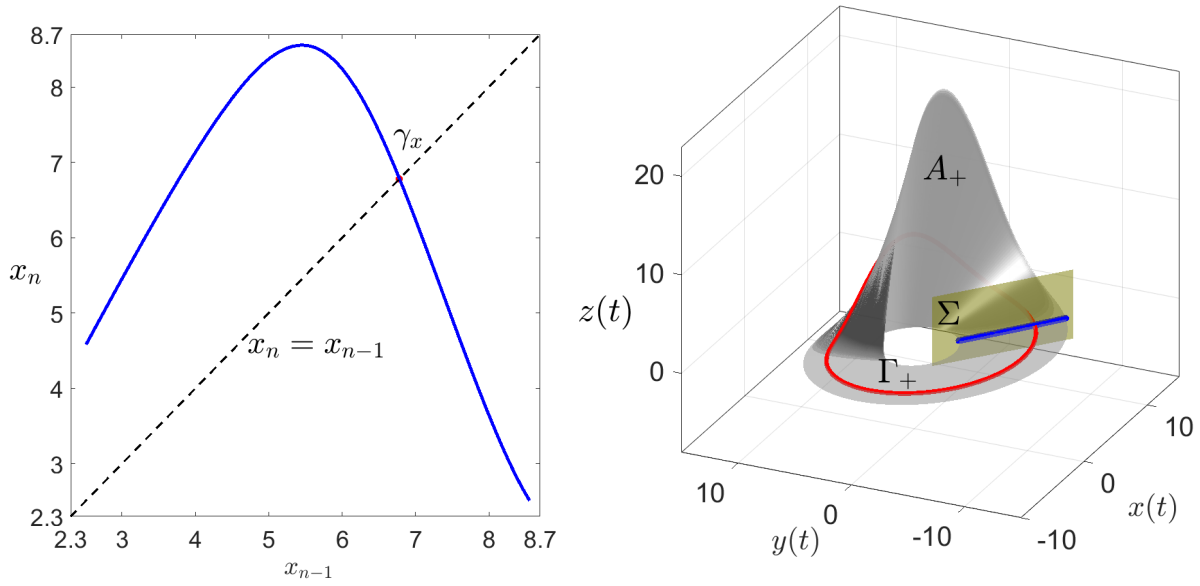

(a) (b)

Figure 6.5: Poincaré section (a) and the projection of x-component of the return map of Rössler system (b) for $a = b = 0.2$ and $c = 5.7$. Assuming that a trajectory $(x(t), y(t), z(t))$ intersect with Σ at $t = t_n$ for $n = 1, 2, ...$, we define $x_n = x(t_n)$. γ_x represents the intersection of the periodic orbit Γ_+ with the section Σ.

applied to the return map of Rössler system. Feigenbaum [18] proved that for one-dimensional maps on some real interval, period-doubling cascades appear in a universal pattern leading to chaotic behaviour. Feigenbaum (bifurcation) diagrams are well known for describing this kind of behaviour for unimodal maps. Figure 6.6 shows such a Feigenbaum diagram for the Rössler return map.

In fact, applying Feigenbaum theory to the Rössler system suggests that there are infinitely many unstable periodic orbits with in a chaotic Rössler attractor. In other words, Rössler attractor is non-minimal invariant set that has proper invariant subsets, that are periodic orbits. In this section we apply a parameter shift to Rössler system (6.4) such that the past limit system has an equilibrium attractor whilst the future limit system has the chaotic attractor A_+. We find, it is possible to have codimension-one heteroclinic connections between the past equilibria and one of the unstable periodic orbits that are densely embedded in A_+. Such a heteroclinic connection, if it exists, means the system exhibits weak tracking.

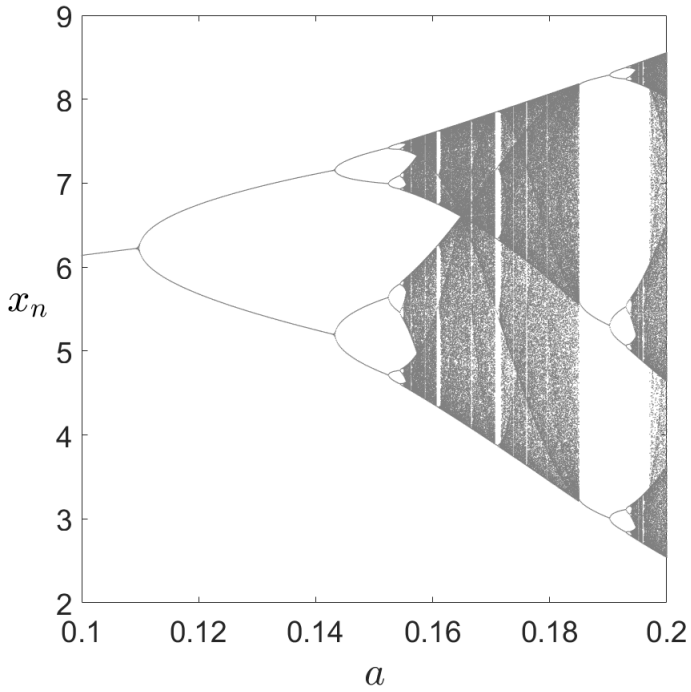

Figure 6.6: The bifurcation diagram of Rössler return map on varying a from 0.1 to 0.2. The other parameters are fixed $b = 0.2$, $c = 5.7$. For every value of $a \in [0.1, 0.2]$, we start at an arbitrary initial condition (x_0, z_0) and calculate $\{(x_n, z_n) : n = 1, 2, ..., N\}$ for N arbitrarily large. We through out the first 100 and plot the rest against a. Note that for each value of a we have $N - 100$ points that are fairly close to the attractor of the map. It can be seen that the first component x_n behaves as if it were a map going through period-doubling bifurcations that lead eventually to a chaotic behaviour.

6.2.2 Rössler system with parameter shift

In this section we shift a from $a_{\min}$ to $a_{\max}$ for some $a_{\min}, a_{\max} \in \mathbb{R}$. Namely,

$$a(rt) = \frac{\Delta}{2}\left(\tanh\left(\frac{\Delta rt}{2}\right) + 1\right) - a_{\min},$$

where $\Delta = a_{\max} - a_{\min}$, $r > 0$ and $a_{\min}$ ($a_{\max}$) are the minimum (maximum) value of the parameter shift a. Throughout this chapter's computations we fix $a_{\max} = -a_{\min} = 0.2$. Similar to the previous cases of (5.3) and (6.1) we can write the

Rössler system with parameter shift a as an autonomous four-dimensional system:

$$\begin{aligned} \dot{x} &= -y - z, \\ \dot{y} &= x + ay, \\ \dot{z} &= b + z(x - c), \\ \dot{a} &= r(a - a_{\min})(a_{\max} - a). \end{aligned} \tag{6.5}$$

The equilibrium, $Z_- = \frac{c-\sqrt{c^2-4ab}}{2a}(a, -1, 1) \approx (-0.007, 0.0351, -0.0351)$, for the past limit system (where $a = -0.2$) is asymptotically stable. The future limit system, on the other hand, has a chaotic attractor A_+ that is the typical Rössler attractor in Figure 6.4.

According to Theorem 3.2.1, for any $r > 0$ system (6.5) must have a pullback attracting solution $\mathcal{A}^{[a,r,Z_-]}$. Our observation suggests that for almost every small enough $r > 0$, the upper forward limit $A_{-\infty}^{[a,r,Z_-]}$ of the pullback attractor $\mathcal{A}^{[a,r,Z_-]}$ is the whole chaotic attractor A_+. Nevertheless, there is a set of isolated values of $r > 0$ that allows $\mathcal{A}^{[a,r,Z_-]}$ to end up tracking one of the unstable periodic orbits that are densely embedded in A_+. In the following discussion we consider one specific periodic orbit Γ_+, which is the period one orbit that is shown in Figure 6.5. However, similar arguments can be made for any period-n orbits that are contained in A_+.

In order to show that there are values of r such that $\mathcal{A}^{[a,r,Z_-]}$ limits to Γ_+ as $t \to \infty$ we approximate the parameter shift $a(rt)$ by the following piecewise linear function $\hat{a}(rt)$:

$$\hat{a}(s) = \begin{cases} a_{\min} & s \in (-\infty, -\tau), \\ \mathrm{m}s + \mathrm{c} & s \in [-\tau, \tau], \\ a_{\max} & s \in (\tau, \infty). \end{cases}$$

where $\mathrm{m} = \Delta/2\tau$,$\mathrm{c} = (a_{\min} + a_{\max})/2$, and $\tau = (\log(\Delta - \delta) - \log(\delta))/\Delta$ for small enough $\delta > 0$. Note that at time $\pm\tau$ the value of a is δ close to the upper and lower

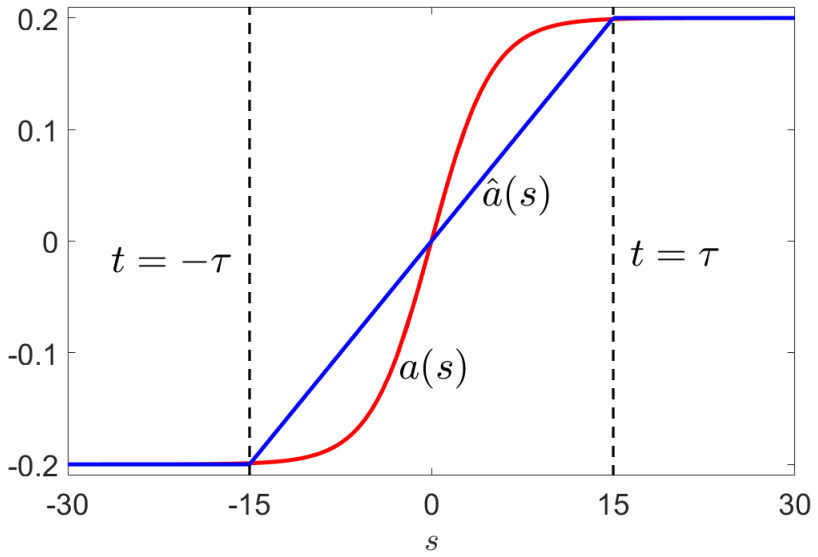

Figure 6.7: The parameter shift $a(s)$ and the piecewise linear approximation $\hat{a}(s)$ vs time, for $a_{\min} = -a_{\max} = 0.2$ and $\delta = 0.001$.

limits. i.e $a(\tau) = a_{\max} - \delta$ and $a(-\tau) = a_{\min} + \delta$, see Figure 6.7. The reason here is that at a finite time $t = \tau$ the system becomes autonomous and so has the chaotic Rössler attractor A_+. Assume that t^* is any real value that satisfies (i) $t^* \geq \tau$ and (ii) $A_{t^*}^{[a,r,Z_-]} \in \Sigma$, where $A_{t^*}^{[a,r,Z_-]}$ is the t^*-fiber of $\mathcal{A}^{[\hat{a},r,Z_-]}$. Note that $A_{t^*}^{[\hat{a},r,Z_-]}$ is a point that belongs to Σ.

The intersection of Γ_+ with Poincaré section is a fixed point γ for the return map. If for some $r = r_c$, $A_{t^*}^{[\hat{a},r,Z_-]}$ happens to be one of the pre-images of γ, then the the upper forward limit of limit of $\mathcal{A}^{[\hat{a},r,Z_-]}$ is Γ_+ and r_c is called a critical rate of weak tracking.

Despite the other periodic orbits that are embedded in A_+, even for just one periodic orbit Γ_+, our numerics show that there are infinitely many critical rates that give EtoP connection for (6.5) and hence weak tracking. Actually, the set of all critical rates r_c should have the same properties as the set of preimages of γ, which we conjecture it is dense and has zero Lebesgue measure. Ád

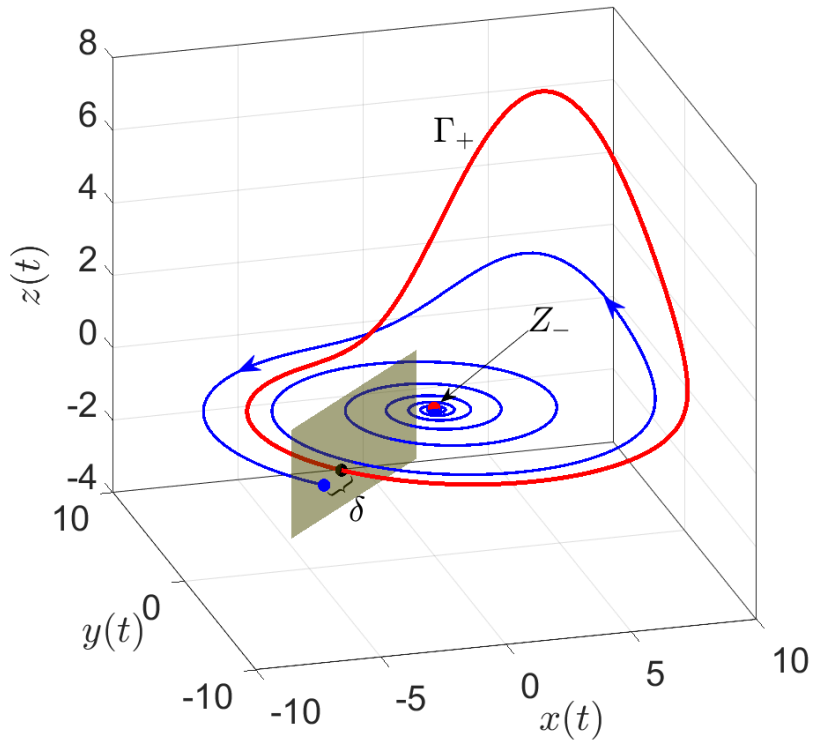

Figure 6.8: A schematic diagram of the shooting method we use to find the the connection between Z_- and Γ_+ for (6.5).

6.2.3 Density of critical rates: numerical evidence

Although Lin's method can be a reliable and robust approach for finding EtoP connections [29, 34], computing and numerically treating projection boundary conditions for Γ_+, similar to (5.10), is not straightforward, as the unstable/center manifolds $W^{u/s}(\Gamma_+)$ are much more complicated than the case of system (5.3). Instead, we use a shooting method with less computational cost. We describe our method as the following:

(i) We approximate the pullback attractor $\mathcal{A}^{[a,r,Z_-]}$ by integrating (6.5), subject to an initial condition p_{init} fairly close to Z_-. Namely, we choose $p_{\text{init}} = (-0.007, 0.035, -0.035)$. The integration time is from -30 to T, where T is large enough to pass the delay in the dynamic bifurcations.

(ii) The pullback attracting solution can be given as $A_t^{[a,r,Z_-]} = (\tilde{x}(t), \tilde{y}(t), \tilde{z}(t))$,

where $t \in [-30, T]$.

(iii) We define a poincaré section Σ.

$$\Sigma := \{(x, y, z) \in \mathbb{R}^3 : x = y \text{ and } x \leq 0\}$$

(iv) Assume that $\mathcal{A}^{[a,r,Z_-]}$ intersects Σ at times $t_n \leq T$ for $n = 1, 2, ..., N$, $N \in \mathbb{N}$ and $t_{n-1} < t_n$.

(v) Consider the last intersection point $(\tilde{x}(t_N), \tilde{y}(t_N), \tilde{z}(t_N))$ and define the following gap function $\eta : \mathbb{R}^2 \to \mathbb{R}$

$$\eta(r) := \frac{\Big((\tilde{x}(t_N), \tilde{z}(t_N)) - \gamma\Big) v_{st}^T}{v_{st} v_{st}^T},$$

where γ is the fixed point of Rössler return map, see Figure 6.5. Note that in addition to r, η depends on T,$b, c, a_{\min}$, $a_{\max}$ and p_{init}. However, we fix all of them throughout and only allow r to vary.

(vi) In analogy to Section 6.2.2, whenever $\eta(r_c) = 0$ we have $\mathcal{A}^{[a,r,Z_-]}$ intersect the stable manifold of Γ_+, which gives the desired EtoP connection. In other words, $\mathcal{A}^{[a,r,Z_-]}$ weakly tracks A_+ at $r = r_c$. The method is illustrated schematically in Figure 6.8.

The function η is as smooth as the state variables of (6.5), i.e. it is at least C^1. Consequently, one can find its roots, and hence the critical rates of weak tracking, numerically by root-finding algorithms such as Newton-Raphson iteration and bisection method. Figure 6.9 shows that system (6.5) exhibit weak tracking at two different critical rates.

Moreover, our numerical investigation is aligned with the argument we make in Section 6.2.2, both of them suggest that there are infinitely many critical rates that give weak tracking for (6.5). In Figure 6.10 we plotted η against $0.9 \leq r \leq 1$, for

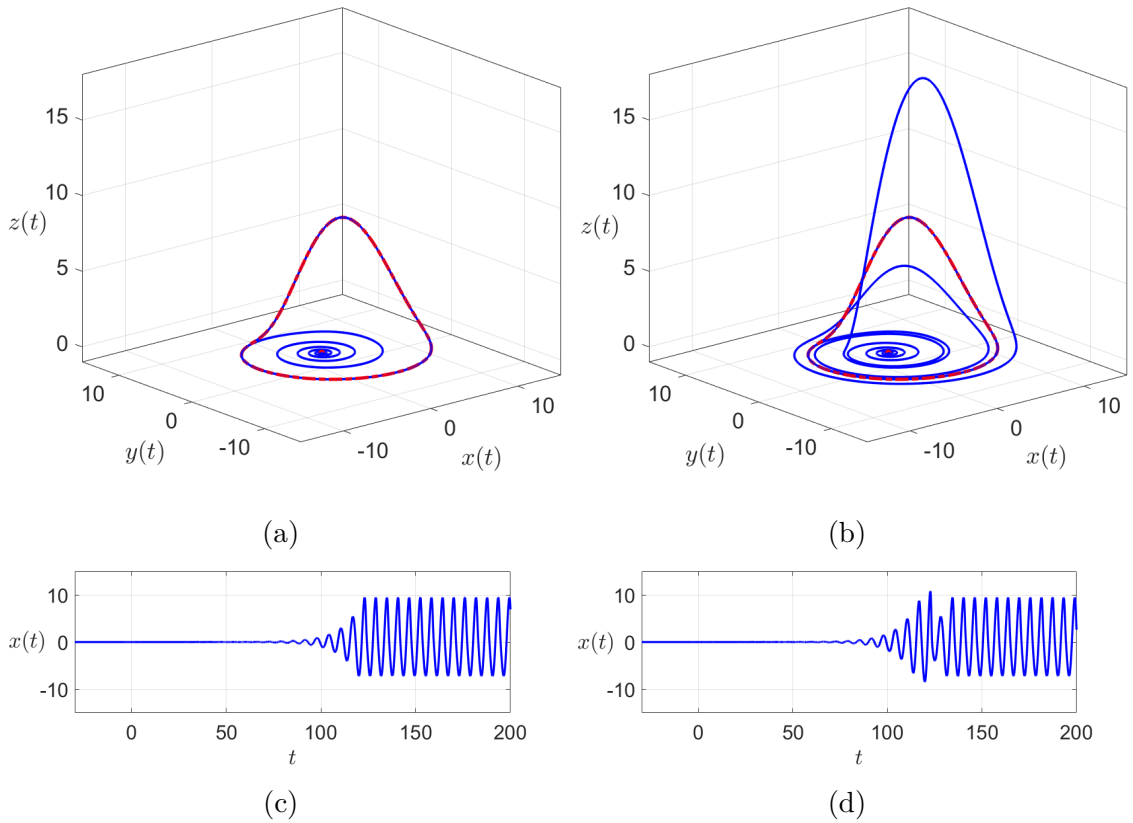

Figure 6.9: Two examples of weak tracking (EtoP connection) for (6.5). The parameters are $b = a_{\max} = -a_{\min} = 0.2$,$c = 5.7$ and $T = 200$. (a) and (c) show the EtoP connection at $r = 0.9202212159423$, (b) and (d) show the connection at $r = 0.995651959127$.

different values of $T = 280$, 300, 320 and 340. The results show that as T increases the number of η's roots increases quite rapidly.

We point out some numerical difficulties. First, there is a large delay in Hopf bifurcation that forces us to choose fairly big integration time T in our calculations, and increases the numerical cost. Delay in dynamic bifurcations is very common and not easy to avoid. For a system with linearly changing time-dependent parameter with slope r, dynamic Hopf bifurcation may have a delay time proportional to $1/r$ before fast escape from the curve of unstable equilibria occurs [53, 43]. More details of dynamic bifurcations and their delay can be found in [9, Chapter 2].

Secondly, It is not obvious how to determine the last intersection of $A_t^{[a,r,Z_-]}$ with the section Σ numerically. The way we do it is that consider a trajectory

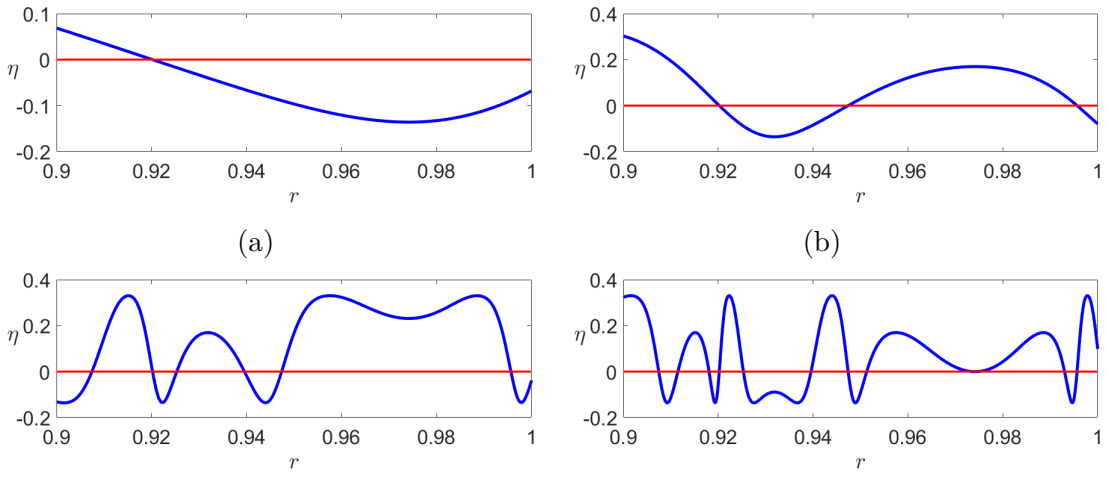

Figure 6.10: The roots of η for different integration time T. (a) $T = 125$, (b) $T = 135$, (c) $T = 145$, and (d) $T = 155$. It can be seen that the zeros of η increase as T increases. Note that, the zeros of η correspond to critical rates that give weak tracking. The parameter values are $b = a_{\max} = -a_{\min} = 0.2$ and $c = 5.7$.

$A_t^{[a,r,Z_-]} = (x(t), y(t), z(t))$ of (6.5). We define a function $\sigma : \mathbb{R} \to \mathbb{R}$ such that $\sigma(t) = x(t) + y(t)$. Any zero of σ gives a time t_0 at which $A_t^{[a,r,Z_-]}$ intersects Σ. We find the roots of σ by Newton-Raphson iteration and choose their maximum. However, solving $\sigma(t) = 0$ in some cases gives unrealistic results, such that $t_0 > T$ although $x(t)$ and $y(t)$ numerically defined for $t \in [-30, T]$. Therefore, a careful choices of the initial guesses are required.

Finally, Figure 6.10 shows that η is smooth with respect to r for a particular range of r, which is $[0.9, 1]$. However, there is no grantee that η is smooth or even continuous for finite T. The definition of η depends on the maximum intersection time which depends on the integration time T. Nevertheless, T can be chosen to smooth η out for any range of r.

Chapter 7

Discussions

7.1 Summary and conclusions

In this thesis, we examine rate-induced phenomena for general compact attractors in the setting of parameter shift systems. Rate-induced phenomena are qualitative changes in the behaviour of a system due to a critical rate of variation for a time-dependent parameter. We consider the class of parameter shift systems where a time-dependent parameter is asymptotic to its upper and lower bounds, both forward and backward in time. This means the system limits to different autonomous systems.

For this class of systems, there is an established theory of tipping points from equilibria [4, 5, 57]. However, for general compact attractors, such as periodic orbits or chaotic attractors, there remains much to be understood. For parameter shift system that limit to systems with compact local attractors, we have tackled the following questions:

(i) How is the local behaviour of the system related to the behaviour of its associated autonomous systems?

(ii) Do the nonautonomous attractors of the systems, namely pullback attractors, have any role to play in describing rate-dependent transitions?

(iii) For a system with periodic orbit attractors, how should one best define and calculate the critical rates of rate-induced transitions?

(iv) Is there a general condition that the system needs to satisfy in order to exhibit weak tracking?

In Chapter 4, we discuss properties of local pullback attractors. Theorem 4.2.2 states that for any asymptotically stable attractor of the past limit system there is a pullback attractor for (1.3) whose upper backward limit is contained within that attractor. Moreover, we show that this pullback attractor tracks a branch of exponentially stable attractors for the associated autonomous systems. Theorem 4.3.1 shows that for a range of small values of $r > 0$ the upper forward limit of the pullback attractor is the same. Nevertheless, there might be a critical value $r_c > 0$ where the tracking is no longer in presence.

In addition to the tracking behaviour that Theorem 4.3.1 shows, Definition 4.3.1 introduces four new rate-dependent phenomena. Assume that we have a local pullback attractor $\mathcal{A}^{[\Lambda,r,A_-]}$ for (1.3) with upper forward limit $A_{+\infty}^{[\Lambda,r,A_-]}$ and suppose for some $r_c > 0$ we have $A_{+\infty}^{[\Lambda,r,A_-]} \subset A_+$ for $r \in (0, r_c)$. Then there is:

(i) *weak tracking*: if $A_{+\infty}^{[\Lambda,r,A_-]}$ is a proper subset of A_+ for some $r > r_c$,

(ii) *partial tipping*: if $A_{+\infty}^{[\Lambda,r,A_-]}$ is not contained in A_+ but intersects it with nonempty set for some $r > r_c$,

(iii) *total tipping*: if the intersection of $A_{+\infty}^{[\Lambda,r,A_-]}$ with A_+ is empty set for some $r > r_c$,

(iv) *invisible tipping*: if for some isolated values of $r_0 > 0$ there is partial tipping but for any $r > r_0$ of $r < r_0$ there is tracking.

Chapter 5 illustrates three of the aforementioned rate-induced phenomena with an example that has a branch of exponentially stable periodic orbits. Namely, system

(5.3) exhibits partial tipping, total tipping, and invisible tipping. We show that the critical rates of these phenomena are associated with codimension-one (PtoE) or (PtoP) connections. We use Lin's method to calculate and continue the critical thresholds and the associated connections in two parameter plane. We also verify our computations by using direct shooting method. The results from the two different approaches match each other quite well.

The (a, r)-parameter plane (Figure 5.4) shows that the upper parts of regions III and IV of partial tipping thin out for $a > 0.15$. We explain this as follows: the threshold of partial and total tipping get close together because of the fold of limit cycles and the PtoE connection curve is trapped between these. Even for relatively large rates the connection between Γ^s_- and Z_+ is associated with partial tracking (partial tipping). Furthermore, as $a \to 0.25$, $\|R_s - R_u\| \to 0$ which means it became very difficult for the pullback attractor $\mathcal{A}^{[\Lambda, r, \Gamma^s_-]}$ to track the branch $\Gamma^s(\Lambda(rt))$ even for very small $r > 0$ (i.e as $a \to 0.25$, $r_1 \to 0$ as well as $\|r_1 - r_2\| \to 0$).

In Chapter 6 we argue that weak tracking requires a sense of nonminimality for the attractors of the future limit system. We present two examples that exhibit weak tracking. System (6.1) is non-generically designed to have non-minimal attractors for the past and the future limit systems. For this settings, we show that there is a range of $r > 0$ where the system undergoes weak tracking. The second example is the well known Rössler system (6.4) with parameter shift. We monotonically shift the bifurcation parameter a such that the system has an equilibrium attractor for the past limit system and chaotic attractor for the future limit system. We then argue that there are isolated critical rates that allow the pullback attractor of the system to end-up tracking an embedded saddle periodic orbit in the future chaotic attractor. We use a novel numerical approach, based on shooting method and carefully chosen Poincaré section, to approximate these critical rates. Furthermore, our investigations suggest that the set of critical rates is dense in $\mathbb{R}$ but with zero Lebesgue measure.

7.2 Remarks for future work

Although our results in Chapter 4 state that parameter shift systems, in general, exhibit tracking along branches of uniformly stable attractors, regardless of how complicated their local pullback attractors are, it does not provide any necessary conditions for the occurrence of any of the rate-dependent phenomena. For example, [4, Theorem 3.2] discusses such necessary conditions for R-tipping from a pullback attracting solutions. If one wants to extend this particular result to general pullback attractors then the concept of forward basin stability for general compact attractors needs to be considered.

Krauskopf and Rieß [34] provide an AUTO example of calculating and continuing PtoP heteroclinic connections. We think that adapting this example for computing the critical rates of system (5.3) would be less time consuming and maybe would give more optimised results. However, we did not get to do that due to some technical problems. Moreover, we point out a numerical difficulty in computing the critical rates for (5.3) and continue them in (r, a)-plane is the integration time T in (5.9, 5.12) needs to be chosen to be proportional to $1/a$ near the Hopf ($a = 0$) and $1/r$ near the fold of limit cycles ($a = 0.25$) to resolve the details. Hence, for any fixed T we find errors in PtoE and PtoP connections in regions close to $a = 0$ and 0.25.

Our example in Chapter 5 has S^1 symmetry. We think systems with periodic orbit attractors and different symmetries may exhibit even richer behaviour. Furthermore, the results of Chapter 4 apply for general non-monotonic parameter shifts. In Chapters 5 and 6 we only use monotonic parameter shift. Considering non-monotonic parameter shift may will give further scenarios of tracking/tipping. For example, there might be a range of rates where the pullback attractor tracks, but for slightly smaller rates it tips partially or totally. This particular scenario has been observed in a system with pullback attracting solutions [4].

This thesis deals with deterministic nonautonomous systems. However, real-world systems usually include noise. There are some benefits for studying rate-

dependent phenomena for noisy systems, one of these is that sudden changes in the properties of noise might be considered as early warning signals for potential transitions [63].

In the presence of noise, Early-warning signals are very useful for studying transitions in real-world systems. Hence, studying warning indicators for the new phenomena that we introduce, such as partial tipping and weak tracking would be worthy. Nevertheless, it might be very challenging, as by looking at individual trajectories, it is not possible to determine whether there is partial or total tipping, although it is quite clear if the case is considered set-wise. An attempt has been made by Hoyer-Leitzel *et al* [26] to characterise tipping by looking at FTLEs. If it is possible to approximate FTLEs from time series data then it might be a valuable early warning indicator for partial tipping and weak tracing.

For nonautonomous Rössler system (6.5) we conjecture there is a dense and zero Lebesgue measure set of critical rates that give weak tracking. We show this argument is right if the system has piecewise linear forcing instead of smooth parameter shift. Moreover, our numerical investigations suggest that such dense zero measure set of critical rates exists. However, more work will be needed to prove this. In Section 6.1 we claim that there is a critical rate r_w of weak tracking, at this particular rate value there is a heteroclinic connection between M_-^s and Z_+. This fact could be proved similar to Section 5.2.

Finally, this thesis discusses model systems that are not necessarily applicable to real-world phenomena. However, we believe the transitions that we have found will be observable in some real-world systems. A particular system where one can observe such transitions is the sensorimotor loop of self-organised robots, where control commands may shift the system from one attractor into the basin of attraction of a different one [68, 69], given that the attractor of such systems can be limit cycles or chaotic attractors.

Bibliography

[1] Hassan M. Alkhayuon and Peter Ashwin. Rate-induced tipping from periodic attractors: Partial tipping and connecting orbits. *Chaos: An Interdisciplinary Journal of Nonlinear Science*, 28(3):033608, Mar 2018.

[2] Kathleen T. Alligood, Tim D. Sauer, and James A. Yorke. *Chaos: An Introduction to Dynamical Systems*. Springer, New York, 1996.

[3] Peter Ashwin and Zhen Mei. A Numerical Bifurcation Function for Homoclinic Orbits. *SIAM Journal on Numerical Analysis*, 35(5):2055–2069, oct 1998.

[4] Peter Ashwin, Clare Perryman, and Sebastian Wieczorek. Parameter shifts for nonautonomous systems in low dimension: Bifurcation- and Rate-induced tipping. *Nonlinearity*, 30:2185–2210, 2017.

[5] Peter Ashwin, Sebastian Wieczorek, Renato Vitolo, and Peter Cox. Tipping points in open systems: bifurcation, noise-induced and rate-dependent examples in the climate system. *Phil. Trans. R. Soc. A*, 370:1166–1184, 2012.

[6] Jean-Pierre Aubin and Helene Frankowska. *Set- Valued Analysis*. Birkhäuser, Boston, 1990.

[7] Bernd Aulbach, Martin Rasmussen, and Stefan Siegmund. Invariant manifolds as pullback attractors of nonautonomous differential equations. *Discrete and Continuous Dynamical Systems*, 15(2):579–596, 2006.

[8] Roberto Barrio, Fernando Blesa, and Sergio Serrano. Unbounded dynamics in dissipative flows: Rössler model. *Chaos: An Interdisciplinary Journal of Nonlinear Science*, 24(2):024407, Jun 2014.

[9] Nils Berglund and Barbara Gentz. *Noise-induced phenomena in slow-fast dynamical systems: a sample-paths approach*. Springer Science & Business Media, London, 2006.

[10] D. N. Cheban, P. E. Kloeden, and B. Schmalfuß. The relationship between pullback, forwards and global attractors of nonautonomous dynamical systems. *Nonlinear Dyn. Syst. Theory*, 2(2):125–144, 2002.

[11] D. N. Cheban, Peter E. Kloeden, and Björn Schmalfuß. Pullback attractors in dissipative nonautonomous differential equations under discretization. *Journal of Dynamics and Differential Equations*, 13(1):185–213, 2001.

[12] Predrag Cvitanovic, Roberto Artuso, Ronnie Mainieri, Gregor Tanner, and Gábor Vattay. *Chaos : Classical and Quantum*. ChaosBook.org, 2018.

[13] Constantine M. Dafermos. An Invariance Principle for Semi-Markov Processes. *Journal of Differential Equations*, 1971(9):239–252, 1971.

[14] V. Dakos, M. Scheffer, E. H. van Nes, V. Brovkin, V. Petoukhov, and H. Held. Slowing down as an early warning signal for abrupt climate change. *Proceedings of the National Academy of Sciences*, 105(38):14308–14312, Sep 2008.

[15] Peter Demenocal, Joseph Ortiz, Tom Guilderson, Jess Adkins, Michael Sarnthein, Linda Baker, and Martha Yarusinsky. Abrupt onset and termination of the African Humid Period: Rapid climate responses to gradual insolation forcing. *Quaternary Science Reviews*, 19(1-5):347–361, 2000.

[16] Peter D. Ditlevsen and Sigfus J. Johnsen. Tipping points: Early warning and wishful thinking. *Geophysical Research Letters*, 37(19):2–5, 2010.

[17] Bard Ermentrout. *Simulating, analyzing, and animating dynamical systems: a guide to XPPAUT for researchers and students*, volume 14. SIAM, 2002.

[18] Mitchell J. Feigenbaum. Quantitative universality for a class of nonlinear transformations. *Journal of Statistical Physics*, 19(1):25–52, Jul 1978.

[19] Ulrike Feudel, Alexander N. Pisarchik, and Kenneth Showalter. Multistability and tipping: From mathematics and physics to climate and brain – Minireview and preface to the focus issue. *Chaos: An Interdisciplinary Journal of Nonlinear Science*, 28(3):033501, Mar 2018.

[20] Franco Flandoli and Björn Schmalfuss. Random attractors for the 3d stochastic navier-stokes equation with multiplicative white noise. *Stochastics and Stochastic Reports*, 59(1-2):21–45, Oct 1996.

[21] Malcolm Gladwell. *The Tipping Point: How Little Things Can Make a Big Difference*. Little, Brown and Company, 2000.

[22] Paul Glendinning. *Stability, Instability and Chaos*. Cambridge University Press, 1997.

[23] Philip Hartman and Ryan Eugene. *Ordinary Differential Equations*. Springer, London, 2014.

[24] M. Henon. On the numerical computation of Poincaré maps. *Physica D: Nonlinear Phenomena*, 5(2-3):412–414, sep 1982.

[25] Ale Jan Homburg and Björn Sandstede. Homoclinic and Heteroclinic Bifurcations in Vector Fields. In *Handbook of Dynamical Systems*, volume 3, pages 379–524. 2010.

[26] Alanna Hoyer-Leitzel, Alice Nadeau, Andrew Roberts, and Andrew Steyer. Connections between rate-induced tipping and nonautonomous stability theory. *ArXiv:1702.02955*, (1):1–22, Feb.

[27] Bálint Kaszás, Ulrike Feudel, and Tamás Tél. Death and revival of chaos. *Physical Review E*, 94(6):1–10, 2016.

[28] Bálint Kaszás, Ulrike Feudel, and Tamás Tél. Leaking in history space: A way to analyze systems subjected to arbitrary driving. *Chaos: An Interdisciplinary Journal of Nonlinear Science*, 28(3):033612, Mar 2018.

[29] Vivien Kirk, Bernd Krauskopf, and Wenjun Zhang. How to find a codimension-one heteroclinic cycle between two periodic orbits. *Discrete and Continuous Dynamical Systems*, 32(8):2825–2851, Mar 2012.

[30] P. E. Kloeden and M. Rasmussen. *Nonautonomous Dynamical Systems*. AMS Mathematical surveys and monographs, 2011.

[31] Peter E. Kloeden. Pullback attractors in nonautonomous difference equations. *Journal of Difference Equations and Applications*, 6(1):33–52, 2000.

[32] Peter E. Kloeden, Christian Pötzsche, and Martin Rasmussen. Limitations of pullback attractors for processes. *Journal of Difference Equations and Applications*, 18(4):693–701, Apr 2012.

[33] J. Knobloch and T. Rieß. Lin's method for heteroclinic chains involving periodic orbits. *Nonlinearity*, 23(1):23–54, 2010.

[34] Bernd Krauskopf and Thorsten Rieß. A Lin's method approach to finding and continuing heteroclinic connections involving periodic orbits. *Nonlinearity*, 21(8):1655–1690, 2008.

[35] Christian Kuehn. A mathematical framework for critical transitions: Bifurcations, fastslow systems and stochastic dynamics. *Physica D: Nonlinear Phenomena*, 240(12):1020–1035, 2011.

[36] Christian Kuehn. A Mathematical Framework for Critical Transitions: Normal

Forms, Variance and Applications. *Journal of Nonlinear Science*, 23(3):457–510, Jun 2013.

[37] Yuri Kuznetsov. *Elements of applied bifurcation theorey*. Springer, New York, 2 edition, 1998.

[38] Jeroen S. W. Lamb, Martin Rasmussen, and Christian S. Rodrigues. Topological bifurcations of minimal invariant sets for set-valued dynamical systems. *Proceedings of the American Mathematical Society*, 143(9):3927–3937, Apr 2015.

[39] Timothy M. Lenton. Early warning of climate tipping points. *Nature Climate Change*, 1(4):201–209, 2011.

[40] C. Letellier, P. Dutertre, and B. Maheu. Unstable periodic orbits and templates of the Rössler system: Toward a systematic topological characterization. *Chaos: An Interdisciplinary Journal of Nonlinear Science*, 5(1):271–282, Mar 1995.

[41] Christophe Letellier, Elise Roulin, and Otto E. Rössler. Inequivalent topologies of chaos in simple equations. *Chaos, Solitons and Fractals*, 28(2):337–360, 2006.

[42] Jeremiah Li, Felix X. F. Ye, Hong Qian, and Sui Huang. Time Dependent Saddle Node Bifurcation: Breaking Time and the Point of No Return in a Non-Autonomous Model of Critical Transitions. *ArXiv:1611.09542*, pages 1–23, Nov.

[43] Claude Lobry. Dynamic Bifurcations. In *Dynamic Bifurcations, volume 1493 of Lecture Notes in Mathematics*, pages 3 – 13. Sipringer, Berlin, 1991.

[44] C. M. Luke and P. M. Cox. Soil carbon and climate change: From the Jenkinson effect to the compost-bomb instability. *European Journal of Soil Science*, 62(1):5–12, 2011.

[45] Sabiha Majumder. *Multiple stable states and abrupt transitions in spatial ecosystems Sabiha Majumder*. PhD thesis, Indian Institute of Science, 2017.

[46] John H Mathews and Kurtis D Fink. *Numerical methods using MATLAB*. Prentice-Hall Inc., Upper Saddle River, New Jersey, USA, 2004.

[47] Robert M. May. Thresholds and breakpoints in ecosystems with a multiplicity of stable states. *Nature*, 269(5628):471–477, Oct 1977.

[48] Robert M. May, Simon A. Levin, and George Sugihara. Ecology for bankers. *Nature*, 451(7181):893–894, Feb 2008.

[49] Katherine Meyer. A Mathematical Review of Resilince in Ecology. *Natural Resource Modeling*, 29(3):339–352, Aug 2016.

[50] John Milnor. On the concept of attractor. *Communications in Mathematical Physics*, 99(2):177–195, 1985.

[51] John Milnor. On the concept of attractor: Correction and remarks. *Communications in Mathematical Physics*, 102(3):517–519, 1985.

[52] José Mujica, Bernd Krauskopf, and Hinke M. Osinga. A Lin's method approach for detecting all canard orbits arising from a folded node. *Journal of Computational Dynamics*, 4(1):143–165, 2017.

[53] Anatoly Neishtadt. On stability loss delay for dynamical bifurcations. *Discrete and Continuous Dynamical Systems - Series S*, 2(4):897–909, Sep 2009.

[54] N. R. Nene and A. Zaikin. Gene regulatory network attractor selection and cell fate decision: insights into cancer multi-targeting. *Proceedings of Biosignal*, pages 14–16, 2010.

[55] Lawrence Perko. *Differential equations and dynamical systems.* Springer Science & Business Media, 2013.

[56] Clare Perryman and Sebastian Wieczorek. Adapting to a changing environment: non-obvious thresholds in multi-scale systems. *Proceedings of the Royal Soci-*

ety A: Mathematical, Physical and Engineering Sciences, 470(2170):20140226–20140226, Aug 2014.

[57] Clare G Perryman. *How Fast is Too Fast? Rate-induced Bifurcations in Multiple Time-scale Systems*. PhD thesis, University of Exeter, 2015.

[58] Martin Rasmussen. *Attractivity and bifurcation for nonautonomous dynamical systems*, volume 1907. Springer, Berlin, 2007.

[59] Martin Rasmussen. Bifurcations of asymptotically autonomous differential equations. *Set-Valued Analysis*, 16(7-8):821–849, 2008.

[60] Martin Rasmussen. Finite-time attractivity and bifurcation for nonautonomous differential equations. *Differential Equations and Dynamical Systems*, 18(1-2):57–78, 2010.

[61] Paul Ritchie. *Early-warning indicators for tipping points*. PhD thesis, University of Exeter, 2016.

[62] Paul Ritchie, Ozkan Karabacak, and Jan Sieber. Inverse-square law between time and amplitude for crossing tipping thresholds. *ArXiv:1709.02645*.

[63] Paul Ritchie and Jan Sieber. Early-warning indicators for rate-induced tipping. *Chaos: An Interdisciplinary Journal of Nonlinear Science*, 26(9):093116, Sep 2016.

[64] Paul Ritchie and Jan Sieber. Probability of noise- and rate-induced tipping. *Physical Review E*, 95(5):052209, May 2017.

[65] Francesco Romano and Christian Kuehn. Analysis and Predictability for Tipping Points with Leading-Order Nonlinear Terms. *ArXiv:1805.00534*, pages 1–13, May 2018.

[66] Otto E. Rössler. An equation for continuous chaos. *Physics Letters A*, 57(5):397–398, 1976.

[67] Otto E. Rössler. Different Types of Chaos in Two Simple Differential Equations. *Zeitschrift für Naturforschung A*, 31(12):1664–1670, Jan 1976.

[68] Bulcsú Sándor, Tim Jahn, Laura Martin, and Claudius Gros. The Sensorimotor Loop as a Dynamical System : How Regular Motion Primitives May Emerge from Self-Organized Limit Cycles. 2(December):1–9, 2015.

[69] Bulcsú Sándor, Michael Nowak, Tim Koglin, Laura Martin, and Claudius Gros. Kick control : using the attracting states arising within the sensorimotor loop of self-organized robots as motor primitives. *Prepreint*, 2018.

[70] Marten Scheffer. *Critical transitions in nature and society*. Princeton University Press, 2009.

[71] Marten Scheffer, Jordi Bascompte, William A. Brock, Victor Brovkin, Stephen R. Carpenter, Vasilis Dakos, Hermann Held, Egbert H. van Nes, Max Rietkerk, and George Sugihara. Early-warning signals for critical transitions. *Nature*, 461(7260):53–59, 2009.

[72] Marten Scheffer, Egbert H. Van Nes, Milena Holmgren, and Terry Hughes. Pulse-driven loss of top-down control: The critical-rate hypothesis. *Ecosystems*, 11(2):226–237, 2008.

[73] H. J. Schellnhuber. Tipping elements in the Earth System. *Proceedings of the National Academy of Sciences*, 106(49):20561–20563, 2009.

[74] George R Sell. Nonautonomous Differential Equations and Topological Dynamics I. The Basic Theory. *Transactions of the American Mathematical Society*, 127(2):241–262, 1967.

[75] George R Sell. Nonautonomous differential equations and topological dynamics. II. Limiting equations. *Transactions of the American Mathematical Society*, 127(2):263–263, Feb 1967.

[76] Steven H. Strogatz. *Nonlinear dynamics and chaos: with applications to physics, biology, chemistry, and engineering.* CRC Press, 2000.

[77] J. M. T. Thompson and Jan Sieber. Climate tipping as a noisy bifurcation: A predictive technique. *IMA Journal of Applied Mathematics (Institute of Mathematics and Its Applications)*, 76(1):27–46, 2011.

[78] J. M. T. Thompson and Jan Sieber. Predicting Climate Tipping As a Noisy Bifurcation: a Review. *International Journal of Bifurcation and Chaos*, 21(02):399–423, 2011.

[79] Egbert H. van Nes, Babak M.S. Arani, Arie Staal, Bregje van der Bolt, Bernardo M. Flores, Sebastian Bathiany, and Marten Scheffer. What Do You Mean, 'Tipping Point'? *Trends in Ecology & Evolution*, 31(12):902–904, Dec 2016.

[80] S. Wieczorek, P. Ashwin, C. M. Luke, and P. M. Cox. Excitability in ramped systems: the compost-bomb instability. *Proceedings of the Royal Society A: Mathematical, Physical and Engineering Science*, 467(2129):1243 –1269, 2011.

[81] Wanfeng Yan, Ryan Woodard, and Didier Sornette. Diagnosis and prediction of tipping points in financial markets: Crashes and rebounds. *Physics Procedia*, 3(5):1641–1657, 2010.